Check for
updates

Effect of fear and delay on a prey-predator model with predator harvesting

Prahlad Majumdar[1] · Bapin Mondal[1] · **Surajit Debnath[1] · Susmita Sarkar[1] ·**
Uttam Ghosh[1]

Abstract
The relationship between prey and predator has been modelled, analysed from the early nineteenth century by considering different types of functional responses and ecological effects. Harvesting of predator in a prey-predator system for controlling their dynamics has been receiving considerable attention from both ecological and economical points of view. A lot of theoretical work has been done on harvesting and reveals that harvesting has a significant impact due to its ecological and economical importance. The fear of prey due to the appearance of predators in the ecological system also plays an important role in drawing the shape of the dynamics of the interacting system. Another important fact, in reality, the reproduction of predator is not instantaneous after the consumption of prey. A constant time lag is necessary for each organism. In this paper, we have investigated the dynamics of a delayed prey-predator model with Holling type III functional response and fear of prey in the natural birth rate. The predator is assumed to be economically significant and harvested linearly. The positivity, boundedness, local stability of equilibrium points and local bifurcation (Transcritical, Hopf bifurcation) of the non-delayed system is established here. We have discussed the local and global stability of the interior equilibrium point in presence of delay. In terms of the delay parameter, the system undergoes through a Hopf bifurcation and we determine in which direction the Hopf bifurcation will go. We carried out some numerical simulations illustrate the theoretical findings using the MAPLE and MATLAB software. Finally, we have drawn some concluding remarks.

Communicated by Rafael Villanueva.

✉ Bapin Mondal
  bapinmondal1@gmail.com

1 Department of Applied Mathematics, University of Calcutta, Kolkata 700009, India

1 Introduction

The interaction between prey and predator is an important issue in bio-mathematical modeling. The first mathematical model was proposed by Malthus (1872) considering the fact that the population expansion rate is directly proportional to the present population density. But this model was unable to convey the appropriate prediction in the real-life scenario because of its unbounded solution. Then introducing the logistic growth function the interaction model was proposed by Lotka (1925) and Volterra (1926) independently to describe the dynamics of the prey-predator model and competition model respectively. After this a large number of research works have been done in this field considering different types of ecological effects (Collings 1997; Panja 2019; Baek 2010; Sarkar and Khajanchi 2020; Zhanga et al. 2019). Among them, the most important effects are the consumption mechanism of prey by the predator which is also known as the functional response (Holling 1965; May 2001; Murray 2002; Freedman 1980; Mondal et al. 2022a, b; Ghosh et al. 2021), fear of prey due to predator (Wang et al. 2016), Allee (Debnath et al. 2019), harvesting (Majumdar et al. 2021) etc. The functional response may be the function of both prey and predator density or only the prey density of the populations (Gupta et al. 2015). Depending on the availability of prey Holling (1965) defined three types of functional responses, namely: the Holling type I, II and III. A Holling type III functional response occurs at high levels of prey population, almost identical to a Holling type II functional response. For low levels of prey species, the number of prey consumed may not follow a linear increase with prey species. Learning time or prey switching or a combination of both can explain this specific response. As prey populations increase, predators' hunting and handling efficiency improve naturally. Predator finds prey so seldom, it has not had enough experience to develop the best ways to capture prey. Holling discovered this mechanism in shrews and deer mice feeding on sawflies (Holling 1959). At low numbers of sawfly cocoons, the per capita growth rate of deer mice follows the exponential rule as the density of cocoons increases, but at a certain density of cocoons, the deer mouse consumption rate reached saturation level as the cocoon density increases. Morozov (2010) demonstrated that Holling type III functional response is suitable for investigating zooplankton feeding on algal blooms in deep-water ecosystems. Prey-predator models with Holling type III functional responses have been tested on phytoplankton-zooplankton-fish by the authors in Dubey et al. (2014). An analysis of phytoplankton-zooplankton system dynamics with harvesting term and Holling III response is presented by Jiang et al. (2018). Using Holling type III functional responses, Kempf et al. (2008) developed a mathematical model of prey-predator interaction to study cod Gadus morhua and whiting Merlangius merlangus population dynamics in the north sea.

The Allee effect in the population is characterized through a positive correlation between the per capita growth rate and the population growth rate at very-low-density (Allee 1931; Biswas 2017; Sen et al. 2014; Ferdy et al. 1999; Wangersky and Cunningham 1957). This type of effect arises in the biological system due to complications in mate finding, reproductive facilitation, inbreeding depression, etc. (Allee 1931; Biswas 2017; Ferdy et al. 1999).

Another important issue in this system is the fear of prey due to predator attack (Wang et al. 2016). Due to the fear from a predator the song sparrows (Melospiza melodia) reduce 40% in offspring reproduction shown by Zanette et al. (2011) in 2001 experimentally. Thus the presence of any predator can affect the birth rate due to anti-predator behaviour more powerfully than direct predation. Also, the fear from a predator may affect the mental condition and physiological condition of juvenile prey. The survivor of adult prey may also be affected due to the fear of the predator. Mathematically, the fear effect was first proposed by

Wang et al. in 2016 Wang et al. (2016). They show that the fear effect has no impact on the stability dynamics of the prey-predator model considering Holling type I functional response. But the fear may stabilize the periodic dynamics when considering Holling type II functional response. Panday et al. (2018) considered a three-species food chain model considering fear in the growth function of prey and middle predator due to the presence of a middle predator and top predator respectively. They have shown that fear can stabilize the chaotic system. Recently a prey-predator model was studied by Kundu et al. (2018) considering discrete-time and fear effect in the prey species.

On the other hand, the prey and predator both are ecological resources, so those can be used for commercial purposes by human society (Onana et al. 2020). For example, the fishery, forestry and wildlife systems are examples of resources that are used by human society's commercial purpose (Das et al. 2009). To study the effect of harvesting mathematically, different types of harvesting policies are used, which are constant, linear and non-linear harvesting.

(I) A constant harvesting function is $H(x, E) = C$, where C is suitable constant (Xiao and Jennings 2005; Peng et al. 2009).

(II) The linear harvesting function is $H(x, E) = qEx$, where q is catchability constant and E is harvesting effort (Zhang et al. 2000; Lenzini and Rebaza 2015).

(III) The non-linear harvesting function is $H(x, E) = \dfrac{qEx}{m_1 E + m_2 x}$, where m_1, m_2 are positive constants (Gupta et al. 2015; Hu and Cao 2017).

It is observed that the linear harvesting function has some unrealistic features such as unbounded prey harvesting and stochastic search for prey. The above unrealistic features are eliminated in the non-linear harvesting function and satisfies the following properties

$$\lim_{E \to \infty} H(x, E) = \frac{qx}{m_1}, \lim_{x \to \infty} H(x, E) = \frac{qE}{m_2}.$$

Thus the non-linear harvesting function shows the saturation properties in terms of inventory abundance and harvesting efforts.

In prey-predator dynamics, the predator population consumes the prey biomass and the energy transfer from one population to another population through the conversion of energy (Biswas 2017; Sen et al. 2014). However, the conversion is not instantaneous, it takes some time for the prey biomass to be converted into predator biomass through a complex mechanism. In every biological phenomenon, there is a mechanism that takes time delay. Using the delay differential equation, we can demonstrate how the delay affects an ecological model. There is a great deal more complexity in the behavior of a delay differential equation than in an ordinary differential equation. The said lag time is known as the delay and if the mechanism is digestion then the delay is also referred to as gestational delay (Lin and Ho 2006). In addition, the logistic growth of the prey incorporates a constant time delay. In ecology, nearly all processes involve time delays, so it will be difficult to come up with a more realistic model if we do not include time lags. Delay is considered in prey species because the prey species take some time τ to produce growth from the food they eat. In ecological modeling, the delay was first introduced by Sen et al. (2014), Wangersky and Cunningham (1957) to address the gestation/maturation delay. A particular observation Kuang makes is that animals take a long time to digest their feed, which delays their activities (Kuang 1993). Using the effect of habitat complexity on delay-induced predator-prey systems, Ma and Wang proposed and analyzed such a system (Ma and Wang 2018).The introduction of delay increases the biological realism of the model, and sometimes the system shows chaotic dynamics.

Authors in Xie and Zhang (2022) examined the effects of dread of predator species on anti-predator behavior in a prey predator system with Holling III type functional responses and prey shelters. They established that fear can stabilize the periodic system. A three-species food chain model was studied by Sk et al. (2022), which included hunting cooperation between predators and prey fear with delay in the system. The authors discover that the fear of the middle predator creates stability while the fear of the top predator creates instability. Our study considers a two-species prey-predator model with fear of prey, predator harvesting and gestation delay in the predator population. Both delayed and non-delayed systems are studied.

Inovation and major contribution of the proposed model are summarized below:

1. The model involves a two-dimensional prey-predator relationship with Holling type III functional response and predation fear to the prey population.
2. We assume that predator populations are economically important and are harvested linearly.
3. Furthermore, gestation delay is considered in order to determine how it affects the richer dynamics.

Finally, the paper is organized in the following way: in Sect. 2, we formulate the mathematical model for prey-predator by introducing the cost of fear and Holling type III functional response for the interacting species. The basic dynamical results such as positivity and boundedness, the existence of the equilibria and their local stability and local bifurcation of the non-delayed system are given in Sect. 3. In Sect. 4, we investigate the several mathematical analysis for delayed system viz., uniform persistence, local and global stability, Hopf bifurcation and stability direction of Hopf bifurcating periodic solution. Also, in Sect. 5, for the purpose of justifying our analytical results, we perform some numerical simulations, which also show that interactions between prey and predator are influenced by the fear effect. Finally, in Sect. 6, we summarize some biological indications from our analytical observation and possible future scope for the upcoming research work.

2 Model formulation

In this paper, we have considered an ecological model having two interacting species, one of them is prey and the other is a predator. We have assumed here that the prey species grows logistically without the presence of any predator. This assumption leads to the following differential equation

$$\frac{\mathrm{d}x(t)}{\mathrm{d}t} = rx(t) - r_0 x(t) - r_1 x^2(t), \text{ with } x(0) = x_0, \tag{1}$$

where $x(t)$ is the prey density at any time t, r is the natural prey birth rate, r_0 is the natural mortality rate and r_1 is the death rate due to the intra-species competition for the prey species.

Now the appearance of any predator in the system affects the prey population. We assume that the predator consumes the prey population according to the prey-dependent Holling type III functional response. Thus the prey-predator system incorporating the Holling type III functional response developed to

$$\frac{\mathrm{d}x(t)}{\mathrm{d}t} = rx(t) - r_0 x(t) - r_1 x^2(t) - \frac{mx^2(t)y(t)}{a + x^2(t)}, \tag{2a}$$

$$\frac{\mathrm{d}y(t)}{\mathrm{d}t} = -dy(t) + \frac{\beta m x^2(t)y(t)}{a + x^2(t)}, \tag{2b}$$

with initial condition $x(0) > x_0$, $y(0) = y_0$; $y(t)$ is the predator density at any time t, d is the natural death rate of a predator, m is the maximum predation rate, a is the environmental protection parameter for the prey population, β is the conversion efficiency of the predator population.

It is observed that the appearance of any predator not only affects the prey species by direct predation. Predator-induced hunting fears the prey species. The survivor of the prey population is highly affected due to predator hunting. The natural birth rate of the prey population reduces due to the predator fear effect. We introduce the fear function $\phi(k, y) = \dfrac{1}{1 + ky(t)}$ (Wang et al. 2016; Debnath et al. 2021; Sk et al. 2022), which is monotonically decreasing function of both k and y, in the prey birth rate r. Then the model system (2) developed as the following

$$\frac{dx(t)}{dt} = \frac{rx(t)}{1 + ky(t)} - r_0 x(t) - r_1 x^2(t) - \frac{mx^2(t)y(t)}{a + x^2(t)}, \tag{3a}$$

$$\frac{dy(t)}{dt} = -dy(t) + \frac{\beta m x^2(t) y(t)}{a + x^2(t)}, \tag{3b}$$

with same initial condition and k is the fear parameter.

The fear functions $\phi(k, y)$ satisfies following biological consequences :

1. $\phi(0, y) = 1$; i.e., if there is no fear in prey due to the predator species, then there will be no loss of reproduction in prey species
2. $\phi(k, 0) = 1$; i.e., as long as predator species do not exist, prey species do not suffer a loss of reproduction.
3. $\lim_{k \to \infty} \phi(k, y) = 0$; i.e., if the fear parameter goes to very large, then prey reproduction ultimately becomes zero.
4. $\lim_{y \to \infty} \phi(k, y) = 0$; i.e., a large predator species density reduces prey reproduction and ultimately eliminates it.
5. $\dfrac{\partial \phi}{\partial k} < 0$; i.e., increased fear of predators leads to a reduction in prey species reproduction.
6. $\dfrac{\partial \phi}{\partial y} < 0$; i.e., increased predator density reduces the reproduction of prey species.

Predator populations are assumed to be economically significant here, and we harvest them. In order to harvest predator populations, we utilize linear harvesting policy. Consequently, when predator hunting is linear, the model system (3) becomes

$$\frac{dx(t)}{dt} = \frac{rx(t)}{1 + ky(t)} - r_0 x(t) - r_1 x^2(t) - \frac{mx^2(t)y(t)}{a + x^2(t)}, \tag{4a}$$

$$\frac{dy(t)}{dt} = -dy(t) + \frac{\beta m x^2(t) y(t)}{a + x^2(t)} - qEy(t). \tag{4b}$$

In a real-life application, every organism needs a constant time lag to reproduce its new program. Keeping this in mind we assume that the reproduction of new prey is not immediate after the prey consumption. We assumed that the predator takes τ time lag for the gestation of prey and the rate of change of predator density depends on the density of prey, predator present at the previous τ time. Thus involving the discrete-time lag the model system (4) reduces to

$$\frac{dx(t)}{dt} = \frac{rx(t)}{1 + ky(t)} - r_0 x(t) - r_1 x^2(t) - \frac{mx^2(t)y(t)}{a + x^2(t)}, \tag{5a}$$

$$\frac{dy(t)}{dt} = -dy(t) + \frac{m\beta x^2(t-\tau)y(t-\tau)}{a + x^2(t-\tau)} - qEy(t), \tag{5b}$$

subject to the following non-negative conditions :

$$x(\theta) = \phi(\theta) \geq 0, \ y(\theta) = \psi(\theta) \geq 0$$
$$\theta \in [-\tau, 0], \ \phi(0) > 0, \ \psi(0) > 0,$$

where $\phi(\theta)$ and $\psi(\theta)$ are bounded continuous functions in the interval $[-\tau, 0]$.

Now we shall establish the positivity, boundedness and persistence of the system which will refers that the system is well-behaved.

3 The model analysis in the absence of delay

In this section, we shall discuss positivity, boundedness of solutions, finding equilibrium points and analysis the local stability of the non delayed system.

3.1 Positivity and boundedness of the solution of the proposed system

In this subsection, we show that positivity of solutions of the non delayed system. After that, we show the boundedness of the solution of the non delayed system. In biological point of view, the positivity of solutions of the system means that the species exist and boundedness means that the species exist finitely. The system (4) can be written as

$$\frac{dx}{dt} = xf_1(x, y), \quad \frac{dy}{dt} = yf_2(x, y) \tag{6}$$

where $f_1 = \dfrac{r}{1 + ky} - r_0 - r_1 x - \dfrac{mxy}{a + x^2}, \quad f_2 = -d + \dfrac{\beta mx^2}{a + x^2} - qE.$

After that, integrating the above equations and using the initial value, we get,

$$x(t) = x_0 \exp\left(\int_0^t [f_1(x(s), y(s))ds]\right) > 0,$$

$$y(t) = y_0 \exp\left(\int_0^t [f_2(x(s), y(s))ds]\right) > 0,$$

with initial conditions $x_0 > 0$ and $y_0 > 0$.

Theorem 1 *The set $\Omega = \{(x, y) : 0 \leq x \leq M_1, \ 0 \leq y \leq M_2\}$ is a region of attraction for all solutions initiating in the positive quadrant, where $M_1 = \dfrac{r}{r_1}$ and $M_2 = \dfrac{(d + r - r_1)^2}{4r_1}$.*

Proof From the first equation of the system (4) we have, $\dfrac{dx}{dt} \leq rx - r_1 x^2$ which implies $\lim\limits_{t \to \infty} \sup x(t) \leq \dfrac{r}{r_1} = M_1$. Now we consider, $P(t) = x(t) + \dfrac{1}{\beta} y(t)$ then differentiating both side of this expression we get,

$$\frac{dP}{dt} = \frac{dx}{dt} + \frac{1}{\beta} \frac{dy}{dt}$$

$$= \frac{rx}{1 + ky} - r_0 x - r_1 x^2 - \frac{d}{\beta} y - \frac{qEy}{\beta}$$

$$\leq rx - r_0x - r_1x^2 - \frac{d}{\beta}y$$

$$\frac{dP}{dt} + dP = (d + r - r_0)x - r_1x^2$$

$$\frac{dP}{dt} + dP \leq \frac{(d + r - r_1)^2}{4r_1}.$$

Hence, we solve the above inequality and using initial conditions we get,

$$P(t) \leq P(0)e^{-dt} + \frac{(d + r - r_1)^2}{4r_1}(1 - e^{-dt}).$$

Moreover, we get $\lim_{t \to +\infty} \sup P(t) \leq \frac{(d + r - r_1)^2}{4r_1} = M_2$, which is independent of the initial condition since, all solutions of the non-delayed system are bounded. □

3.2 Equilibrium points and stability

The equilibrium points of the proposed system (4) are given at the intersection of prey and predator nullclines,

$$xf_1(x, y) = 0, \, yf_2(x, y) = 0.$$

Equilibrium points of our proposed system (4) are:

(i) The trivial equilibrium point $E_0(0, 0)$.

(ii) The prey only (axial) equilibrium point $E_1\left(\frac{r - r_0}{r_1}, 0\right)$.

(iii) Interior or co-existence equilibrium points of the system (4) are positive solutions of $f_1(x, y) = 0$ and $f_2(x, y) = 0$. Let $E^*(x^*, y^*)$ be the interior equilibrium point of the system (4), so $x^* = \left(\frac{qaE + ad}{m\beta - d - qE}\right)^{1/2}$ and y^* is a positive roots of the following equation

$$A_1y^{*2} + A_2y^* + A_3 = 0,$$

where $A_1 = mkx^*$, $A_2 = (mx^* + akr_0 + akr_1x^* + kr_0x^{*2} + kr_0x^{*3})$, $A_3 = ar_0 + ar_1x^* + r_0x^{*2} + r_1x^{*3} - ar - rx^{*2}$.

Here, A_1 and A_2 are positive, so the above equation can have at most only one positive root depending on the sign of A_3, if $A_3 < 0$ then the above equation have one positive root otherwise no positive root of the above equation. So, the above discussion we can conclude that the system (4) have at most one interior equilibrium points.

Here, we shall show that the local stability of the system (4) with time delay $\tau = 0$ by using the eigenvalue linearised method about all the above mentioned equilibrium points.

Theorem 2 *The trivial equilibrium point $E_0(0, 0)$ is locally stable if $r < r_0$ and unstable $r > r_0$.*

Proof Eigenvalues of the Jacobian matrix of the system (4) at trivial point $E_0(0, 0)$ are $r - r_0$ and $-Eq - d$. Here, one eigenvalue is negative and other eigenvalue is negative if $r < r_0$. Hence trivial equilibrium point is stable if $r < r_0$ otherwise unstable. All the species will go extinct when the birth rate is less than the growth rate of the prey population, which is very dangerous in the sub-ecosystem. □

Theorem 3 *The axial equilibrium point* $E_1 \left(\dfrac{r - r_0}{r_1}, 0 \right)$ *is locally asymptotically stable if*

$Eaqr_1^2 + Eqr^2 + Eqr_0^2 + adr_1^2 + 2\beta mrr_0 + dr^2 + dr_0^2 < 2Eqrr_0 + \beta mr^2 + \beta mr_0^2 + 2drr_0$
and unstable if the reverse inequality holds.

Proof Eigenvalues of the Jacobian matrix at the equilibrium point $E_1 \left(\dfrac{r - r_0}{r_1}, 0 \right)$ are $-r + r_0$

and $-\dfrac{(Eaqr_1^2 + Eqr^2 - 2Eqrr_0 + Eqr_0^2 + adr_1^2 - \beta mr^2 + 2\beta mrr_0 - \beta mr_0^2 + dr^2 - 2drr_0 + dr_0^2)}{(ar_1^2 + r^2 - 2rr_0 + r_0^2)}$. Thus the equilib-

rium point is locally asymptotically stable if $Eaqr_1^2 + Eqr^2 + Eqr_0^2 + adr_1^2 + 2\beta mrr_0 + dr^2 + dr_0^2 < 2Eqrr_0 + \beta mr^2 + \beta mr_0^2 + 2drr_0$, otherwise the equilibrium point is unstable. □

Theorem 4 *The interior equilibrium point* $E^*(x^*, y^*)$ *locally asymptotically stable if* $T_{tr} < 0$ *and* $D_{det} > 0$ *holds, where* T_{tr} *and* D_{det} *are defined in the text.*

Proof The variation matrix at $E^*(x^*, y^*)$ is given by

$$J_E^* = \begin{pmatrix} \dfrac{r}{(ky^* + 1)} - r_0 - 2r_1 x^* - \dfrac{2amx^*y^*}{(x^{*2} + a)^2} & -\dfrac{rkx^*}{(ky^* + 1)^2} - \dfrac{mx^{*2}}{(x^{*2} + a)} \\ \dfrac{2ma\beta x^*y^*}{(x^{*2} + a)^2} & \dfrac{m\beta x^{*2}}{(x^{*2} + a)} - d - qE \end{pmatrix}.$$

The trace and determinant values of the variation matrix at the interior equilibrium point are

given by $T_{tr} = tr(J_{E^*}) = \dfrac{r}{(ky^* + 1)} - r_0 - 2r_1 x^* - \dfrac{2amx^*y^*}{(x^{*2} + a)^2} + \dfrac{m\beta x^{*2}}{(x^{*2} + a)} - d - qE,$

and

$$D_{det} = det(J_{E^*}) = \left(\dfrac{r}{(ky^* + 1)} - r_0 - 2r_1 x^* - \dfrac{2amx^*y^*}{(x^{*2} + a)^2} \right) \left(\dfrac{m\beta x^{*2}}{(x^{*2} + a)} - d - qE \right)$$
$$+ \left(\dfrac{rkx^*}{(ky^* + 1)^2} + \dfrac{mx^{*2}}{(x^{*2} + a)} \right) \left(\dfrac{2ma\beta x^*y^*}{(x^{*2} + a)^2} \right).$$

Here the above both the expressions T_{tr} and D_{det} can be positive or negative, so the stability of the system at the interior equilibrium point depends on both expressions T_{tr} and D_{det} of the variation matrix. Therefore, by the theorem of Routh-Hurwitz criterion, the interior equilibrium point is locally asymptotically stable if $T_{tr} < 0$ and $D_{det} > 0$. □

3.3 Local bifurcation analysis

In this subsection, we shall discuss Transcritical and Hopf bifurcation analysis of the system (4). Here, we first discuss Transcritical bifurcation about the trivial equilibrium point $E_0(0, 0)$ with r is the bifurcation parameter. After that, the same bifurcation about axial equilibrium

point $E_1 \left(\dfrac{r - r_0}{r_1}, 0 \right)$ with E as the bifurcation parameter.

Theorem 5 *The system* (4) *admits a transcritical bifurcation for* $E_0(0, 0)$ *at the parameter threshold* $r = r^{[TC]} = r_0$.

Proof The jacobian matrix of the system (4) at the equilibrium point $E_0(0, 0)$ for the parameter value $r^{[TC]} = r_0$ is

$$J \left(E_0; r = r^{[TC]} \right) = \begin{bmatrix} 0 & 0 \\ 0 & -Eq - d \end{bmatrix}.$$

Clearly, the above jacobian matrix have one zero eigenvalue. Now, we find eigenvectors of the above jacobian matrix corresponding the zero eigenvalue. Eigenvectors of the jacobian matrix and its transpose matrix are $v = [1 \quad 0]^t$ and $w = [1 \quad 0]^t$ respectively. Now, we use the Sotomayor's theorem for transcritical bifurcation, then the transversality condition are

$$w^t F_r(E_0; r = r^{[TC]}) = 0$$

$$w^t D F_r(E_0; r = r^{[TC]})v = 1 \neq 0$$

$$w^t D^2 F(E_0; r = r^{[TC]})(v, v) = -2r_1 \neq 0.$$

Since all the transversality conditions are satisfied therefore the system (4) undergoes a transcritical bifurcation at $r = r^{[TC]}$. Biologically, transcritical bifurcation is of great importance. In this case, the system admits a suitable value of prey birth rate (r), below which no species will survive; however, after crossing the critical value of prey growth rate, only prey species will survive. Numerically, we can verify that the system experiences another transcritical bifurcation at the next critical value of r. Here, the predator-free equilibrium point becomes unstable from stable and a stable interior equilibrium point arises i.e., both populations will survive after crossing the second critical value (see Fig. 2). □

Theorem 6 *The system* (4) *admits a transcritical bifurcation for* $E_1 \left(\dfrac{r - r_0}{r_1}, 0 \right)$ *at the*

parameter threshold $E^{[TC]} = \dfrac{(adr_1^2 + \beta mr^2 - 2\beta mrr_0 + \beta mr_0^2 - dr^2 + 2drr_0 - dr_0^2)}{(ar_1^2 + r^2 - 2rr_0 + r_0^2)q}.$

Proof The jacobian matrix of the system (4) at the equilibrium point $E_1 \left(\dfrac{r - r_0}{r_1}, 0 \right)$ for the

parameter value $E^{[TC]} = \dfrac{(adr_1^2 + \beta mr^2 - 2\beta mrr_0 + \beta mr_0^2 - dr^2 + 2drr_0 - dr_0^2)}{(ar_1^2 + r^2 - 2rr_0 + r_0^2)q}$ is

$$J \left(E_1; E = E^{[TC]} \right) = \begin{bmatrix} r_0 - r & \dfrac{(r_0 - r)(akrr_1^2 + kr^3 - 2kr^2r_0 + krr_0^2 + mrr_1 - mr_0r_1)}{r_1(ar_1^2 + r^2 - 2rr_0 + r_0^2)} \\ 0 & 0 \end{bmatrix}.$$

Clearly, from the above jacobian matrix have one zero eigenvalue. Now, we find the eigenvectors of the above jacobian matrix corresponding the zero eigenvalue. The eigenvectors of the jacobian matrix and its transpose matrix are v

$$= \begin{bmatrix} \dfrac{(2kr^2r_0 - krr_0^2 - mrr_1 + mr_0r_1 - akrr_1^2 - kr^3)}{r_1(ar_1^2 + r^2 - 2rr_0 + r_0^2)} & 1 \end{bmatrix}^t \text{ and } w = [0 \quad 1]^t \text{ respectively.}$$

Now we use the Sotomayor's theorem for transcritical bifurcation, then the transversality conditions are

$$w^t F_E(E_1; E = E^{[TC]}) = 0,$$

$$w^t D F_E(E_1; E = E^{[TC]})v = -d \neq 0,$$

$$w^t D^2 F(E_1; E = E^{[TC]})(v, v)$$

$$= \dfrac{2r_1^3 a\beta m(r - r_0)(2kr^2r_0 - krr_0^2 - mrr_1 + mr_0r_1 - akrr_1^2 - kr^3)}{r_1(ar_1^2 + r^2 - 2rr_0 + r_0^2)(ar_1^2 + r^2 - 2rr_0 + r_0^2)^2} \neq 0.$$

Since all the transversality conditions are satisfied, therefore the system (4) undergoes a transcritical bifurcation at $E = E^{[TC]}$. Hence, transcritical bifurcation arises with respect to predator harvesting. There is a critical value of the predator harvesting rate below which

both populations will survive and above which predator population goes to extinction (see Fig. 4). It is clear from the above analysis that moderate harvesting is biologically acceptable but extreme harvesting is venerable for the system. □

In the next theorem, we shall investigate the possibility of Hopf-bifurcation about the interior equilibrium point E^*, taking the fear factor (k) as the bifurcation parameter and keeping other parameters fixed. In this regard, we have the following theorem

Theorem 7 *The necessary and sufficient conditions for the occurrence of Hopf-bifurcation at the interior equilibrium E^* are that there exists a critical value $k = k^{[HB]}$ such that*

(1) $tr(J_{E^*})|_{k=k^{[HB]}} = 0$,

(2) $\left[\dfrac{d Re(\lambda(k))}{dk} \right]_{k=k^{[HB]}} \neq 0$.

Proof The characteristic equation of the system (4) about the interior equilibrium point is given by

$$\lambda^2 + C_1 \lambda + C_2 = 0, \tag{7}$$

where $C_1 = -tr(J_E^*)$ and $C_2 = det(J_E^*)$. Let $\lambda(k) = u(k) + iv(k)$ be the roots of eq. (7). Now, we substituting this value in eq. (7), separating real and imaginary parts, we get

$$u^2 - v^2 + C_1 u + C_2 = 0, \tag{8}$$
$$2uv + C_1 v = 0. \tag{9}$$

A necessary condition for the change of stability of the system (4) through interior equilibrium E^* is that the eq. (7) must have purely imaginary roots. We set $k = k^{[HB]}$ such that $u(k^{[HB]}) = 0$, and put in (8). Then, we have

$$- v^2 + C_2 = 0, \tag{10}$$
$$C_1 v = 0, \; v \neq 0. \tag{11}$$

From Eqs. (10), we have $C_1(k^{[HB]}) = 0$ and $v(k^{[HB]}) = \sqrt{C_2(k^{[HB]})}$, which implies $\lambda((k^{[HB]})) = i\sqrt{C_2((k^{[HB]}))}$. The eigenvalues of equation (7) are

$$\lambda_{1,2} = \frac{-C_1 \pm \sqrt{C_1^2 - 4C_2}}{2}.$$

Here, C_1 and C_2 are the functions of the parameter k, when the value of other parameters are fixed. Moreover, we assume there exists some $k = k^{[HB]}$ such that $C_1(k^{[HB]}) = 0$ and $C_2(k^{[HB]}) > 0$. Therefore, the real parts of these eigenvalues change the sign when k passes through the critical value $k = k^{[HB]}$. Thus, the system switches its stability provided that the transversality condition is satisfied. Differentiating Eqs. (8), (9) with respect to k and put $u = 0$, we have

$$C_1 \frac{du}{dk} - 2v \frac{dv}{dk} = -\frac{dC_2}{dk},$$
$$2v \frac{du}{dk} + C_1 \frac{dv}{dr} = -v \frac{dC_1}{dk}.$$

Solving the above system of equations, we have

$$\left[\frac{d\text{Re}(\lambda(k))}{dk}\right]_{k=k^{[HB]}} = -\left[\frac{2v^2\frac{dC_1}{dk} + C_1\frac{dC_2}{dk}}{C_1^2 + 4v^2}\right]_{k=k^{[HB]}} \neq 0$$

provided $\left[2v^2\frac{dC_1}{dk} + C_1\frac{dC_2}{dk}\right]_{k=k^{[HB]}} \neq 0$.

Having Hopf bifurcation concerning the fear parameter indicates that there is a particular value of the fear parameter at which the system's stability switches (from stable to limit cycle or from limit cycle to stable). Biologically, the Hopf bifurcation threshold parameter values guarantee the persistence of both species in a steady or oscillatory mode for a long time. □

4 Analysis of the model in presence of delay

In this section, we shall discuss the persistence, local stability, Hopf bifurcation and global stability analysis about the interior equilibrium points of the delay system (5).

4.1 Positivity and boundedness of system solutions

In this section, we shall present the condition of positivity and boundedness of the delay system (5). From the first equation of the system (5) we have,

$$\frac{dx}{x} = \left(\frac{r}{1+ky} - r_0 - r_1x - \frac{mxy}{a+x^2}\right)dt.$$

Now integrating both side of the above equation between the limits 0 to t, we get,

$$x(t) = x_0 \exp\left(\int_0^t \left[\frac{r}{1+ky(s)} - r_0 - r_1x(s) - \frac{mx(s)y(s)}{a+x^2(s)}\right]ds\right).$$

And, similarly from the second equation of the delay system (1) we get,

$$y(t) = y_0 \exp\left(\int_0^t \left[-d + \frac{m\beta x^2(s-\tau)y(s-\tau)}{a+x^2(s-\tau)} - qE\right]ds\right),$$

where $x_0 > 0$ and $y_0 > 0$. Therefore, $x(t) > 0$ and $y(t) > 0$.

Lemma 1 *All solutions of the delay system* (5) *starting in* $int(\mathbb{R}_+^2)$ *are uniformly bounded with an ultimate bound.*

Proof The first equation of the delay system (5) we get,

$$\frac{dx}{dt} \leq rx - r_1x^2.$$

Therefore, $\lim_{t\to\infty} \sup x(t) \leq \frac{r}{r_1}$.

Now, defined a function $V = x(t-\tau) + \frac{1}{\beta}y(t)$. After that, taking its time derivative along the solution of the delay system (5), we have

$$\dot{V} = \dot{x}(t-\tau) + \frac{1}{\beta}\dot{y}$$

$$= \frac{rx(t-\tau)}{1+ky(t-\tau)} - r_0 x(t-\tau) - r_1 x^2(t-\tau) - \frac{mx^2(t-\tau)y(t-\tau)}{a+x^2(t-\tau)}$$

$$- \frac{d}{\beta}y + \frac{mx^2(t-\tau)y(t-\tau)}{a+x^2(s-\tau)} - \frac{1}{\beta}qEy$$

$$\leq (d+r-r_0)x(t-\tau) - r_1 x^2(t-\tau)$$

$$\dot{V} \leq -r_0 V + \frac{(d+r-r_1)^2}{4r_1}$$

which given, $\lim_{t\to\infty} \sup V(t) \leq \frac{(d+r-r_1)^2}{4r_0 r_1}$.

Let $M = \max\left(\frac{r}{r_1}, \frac{(d+r-r_1)^2}{4\beta r_1}\right)$. □

Lemma 2 *Here, for any positive solution of system* (5), *the relations* $y(t) \geq y(t-\tau)e^{-d\tau}$ *and* $y(t-\tau) \geq y(t)e^{-m_1\tau}$ *are always satisfied, where* $m_1 = \beta M e^{d\tau}$.

4.2 Local stability and Hopf Bifurcation with delay system about the interior equilibrium point E^*

In this subsection, we shall discuss dynamics of the system in presence of delay.

4.2.1 Local stability and Hopf bifurcation analysis of the delayed model

Now, we will study the local stability of various equilibrium points for the delayed system (5). The Jacobian matrix of the system (5) at any equilibrium point $E(x, y)$ is given by

$$J_E = \begin{bmatrix} \frac{r}{1+ky} - r_0 - 2r_1 x - \frac{2max y}{(a+x^2)^2} & -\left(\frac{rkx}{(ky+1)^2} + \frac{mx^2}{x^2+a}\right) \\ \frac{2ma\beta xy}{(a+x^2)^2}e^{-\lambda\tau} & -d + \frac{m\beta x^2}{a+x^2} - qE \end{bmatrix}.$$

It is obvious that the stability of trivial and axial equilibrium points remain same as in the non-delayed model i.e., the effect of delay has no impact on the stability of trivial and axial equilibrium points.

Let (x^*, y^*) be the only interior equilibrium point of the system (5), using the transformation $X = x - x^*$, $Y = y - y^*$ and Linearizing the system (5) we get

$$\frac{dX}{dt} = b_1 X + b_2 Y, \tag{12a}$$

$$\frac{dY}{dt} = b_3 X(t-\tau) + b_4 Y(t-\tau) + b_5 Y, \tag{12b}$$

where,

$$b_1 = \frac{r}{1+ky^*} - r_0 - 2r_1 x^* - \frac{2max^* y^*}{(a+x^{*2})^2}, \quad b_2 = -\left(\frac{rkx^*}{(ky^*+1)^2} + \frac{mx^{*2}}{x^{*2}+a}\right),$$

$$b_3 = \frac{2ma\beta x^* y^*}{(a+x^{*2})^2}, \quad b_4 = \frac{m\beta x^{*2}}{a+(x^*)^2}, \quad b_5 = -(d+qE).$$

After that we find the characteristic equation of the above linearised system (12) which is given in the following form:

$$\lambda^2 + A_0\lambda + B_0 + (C_0\lambda + D_0)e^{-\lambda\tau} = 0 \tag{13}$$

where, $A_0 = -(b_1 + b_5)$, $B_0 = b_1b_5$, $C_0 = -b_4$ and $D_0 = b_1b_4 - b_2b_3$.

In non-linear delay equation exist two types of stability among them: absolute stability, which is independent on delay and other one conditional stability, which is dependent on delay.

Case - I: $\tau = 0$.

Then the characteristic eq. (13) becomes

$$\lambda^2 + (A_0 + C_0)\lambda + B_0 + D_0 = 0 \tag{14}$$

The interior equilibrium point $E^*(x^*, y^*)$ is locally asymptotically stable if and only if the roots of the eq. (14) have negative real parts, which is true if

(i) $A_0 + C_0 > 0$,
(ii) $B_0 + D_0 > 0$.

Case - II: $\tau \neq 0$.

Let $i\omega$ is a root of the eq. (13), then putting $i\omega$ in 13 separating the real and imaginary parts, we gen in the following form

$$D_0 \cos\omega\tau + C_0\omega \sin\omega\tau = \omega^2 - B_0, \tag{15}$$

$$C_0\omega \cos\omega\tau - D_0 \sin\omega\tau = -A_0\omega. \tag{16}$$

From above two equation we obtain,

$$\omega^4 - (C_0^2 - A_0^2 + 2B_0)\omega^2 + (B_0^2 - D_0^2) = 0, \tag{17}$$

and $\cos\omega\tau = \dfrac{D_0(\omega^2 - B_0 - \omega^2 A_0 C_0)}{\omega^2 C_0^2 + D_0^2}$ and $\sin\omega\tau = \dfrac{\omega C_0(\omega^2 - B_0 + \omega A_0 D_0)}{\omega^2 C_0^2 + D_0^2}$.

From (17), we see that, if

(iii) $(A_0^2 - C_0^2 - 2B_0) > 0$ and $(B_0^2 - D_0^2) > 0$, then the equation (17) does not have any positive roots. So, the characteristic eq. (13) does not have any purely imaginary roots. Since (i) and (ii) secure that all roots of (14) have negative real parts by Rouche's theorem, it follows that the roots of (17) have negative real part too. The abridge of the above discussion is summarize in the following theorem:

Theorem 8 *If the conditions* (i)–(iii) *hold, then all the roots of* (13) *have negative real parts for all* $\tau \geq 0$ *i.e. E^* will be stable.*

On the other hand, if (iv) $(B_0^2 - D_0^2) < 0$, then (17) has a unique positive root ω_0^2.

After that we substitute ω_0^2 into (15) and solving for τ, we get

$$\tau_n = \frac{1}{\omega_0} \arctan\left(\frac{\omega_0 A_0 D_0 + \omega_0 C_0(\omega_0^2 - B_0)}{D_0(\omega_0^2 - B_0) - \omega_0^2 A_0 C_0}\right) + \frac{2n\pi}{\omega_0}, n = 0, 1, 2, 3... \tag{18}$$

If

(v) $(C_0^2 - A_0^2 + 2B_0) > 0$, $(B_0^2 - D_0^2)$, and $(C_0^2 - A_0^2 + 2B_0)^2 > 4(B_0^2 - D_0^2)$, then (17) has two positive roots ω_+^2 and ω_-^2.

Now substituting $\omega_{\pm}^2$ into (14), we get

$$\tau_k^{\pm} = \frac{1}{\omega_{\pm}} \arctan\left(\frac{\omega_{\pm} A_0 D_0 + \omega_{\pm} C_0(\omega_{\pm}^2 - B_0)}{D_0(\omega_{\pm}^2 - B_0) - \omega_{\pm}^2 A_0 C_0} \right) + \frac{2n\pi}{\omega_{\pm}}, n = 0, 1, 2, 3... \quad (19)$$

Now, differentiating the eq. (13) with respect to τ, we get

$$\frac{d\lambda}{d\tau} = \frac{(C_0\lambda^2 + D_0\lambda)e^{-\lambda\tau}}{(2\lambda + A_0) + (C_0 - C_0\lambda\tau - D_0\tau)e^{-\lambda\tau}},$$

$$\left(\frac{d\lambda}{d\tau}\right)^{-1} = \frac{C_0}{\lambda(C_0\lambda + D_0)} - \frac{(2\lambda + A_0)}{\lambda(\lambda^2 + A_0\lambda + B_0)} - \frac{\tau}{\lambda} \quad (20)$$

by using $e^{-\lambda\tau} = -\left(\frac{\lambda^2 + A_0\lambda + B_0}{C_0\lambda + D_0}\right)$.

Thus

$$\text{sign}\left(\frac{d}{d\tau}(Re\lambda)\right)_{\lambda=i\omega} = \text{sign}\left(Re\left(\frac{d\lambda}{d\tau}\right)^{-1}\right)_{\lambda=i\omega}$$

$$= \text{sign}\left(\frac{2\omega^2 - (C_0^2 - A_0^2 + 2B_0)}{C_0^2\omega^2 + D_0^2}\right), \quad (21)$$

by using $(\omega^2 - B_0)^2 + A_0^2\omega^2 = D_0^2 + C_0^2\omega^2$.

Theorem 9 *If* (i), (ii) *and* (iv) *hold, then the interior equilibrium point $E^*(x^*, y^*)$ is asymptotically stable if $\tau < \tau_0$ and unstable $\tau > \tau_0$. Further, if τ increases through the critical value of τ_0, then interior equilibrium point $E^*(x^*, y^*)$ bifurcates with small amplitude periodic solutions, where*

$$\tau_0 = \frac{1}{\omega_0} \arctan\left(\frac{\omega_0 A_0 D_0 + \omega_0 C_0(\omega_0^2 - B_0)}{D_0(\omega_0^2 - B_0) - \omega_0^2 A_0 C_0} \right). \quad (22)$$

Proof The interior equilibrium point $E^*(x^*, y^*)$ is asymptotically stable for $\tau = 0$ if (i) and (ii) hold. From Butler's lemma, we conclude that the interior equilibrium point remain stable for $\tau < \tau_0$. We have to show now

$$\frac{d}{d\tau}(Re\lambda)\Big|_{\tau=\tau_0, \omega=\omega_0} > 0. \quad (23)$$

However, the conditions of Hopf bifurcation of the system are then satisfied the required periodic solution.

Now from (19), we have

$$\text{sign}\left(\frac{d}{d\tau}(Re\lambda)\right)_{\lambda=i\omega_0} = \text{sign}\left(\frac{\sqrt{(C_0^2 - A_0^2 + 2B_0)^2 - 4(B_0^2 - D_0^2)}}{C_0^2\omega_0^2 + D_0^2} \right). \quad (24)$$

Therefore,

$$\frac{d}{d\tau}(Re\lambda)\Big|_{\tau=\tau_0, \omega=\omega_0} > 0. \quad (25)$$

The transversality condition are hold for Hopf bifurcation at $\omega = \omega_0, \tau = \tau_0$. $\qquad\square$

4.3 Global stability of the delay system about the interior equilibrium point E^*

In this section, we shall discuss the global stability of the interior equilibrium point $E^*(x^*, y^*)$ in presence of dealy.

Theorem 10 *The interior equilibrium point $E^*(x^*, y^*)$ of the system* (5) *is Globally asymptotically stable if $\min\{p_1 m_1, p_2 m_2\} > 0$ where p_1*

$$= \left(r_1 - \frac{m(a + x^{*2})y^*}{(a + m_1^2)(a + x^{*2})} - \frac{(1 + kM_2)}{(1 + km_2)(1 + ky^*)} - (a^2 + \tau) \frac{2M_1^2 \beta m}{a(a + x^{*2})} \right) \text{ and } p_2 =$$

$$\left(\frac{km_1}{(1 + kM_2)(1 + ky^*)} - \frac{m(a + x^{*2})x^*}{(a + m_1^2)(a + x^{*2})} \right) \text{ and } m_1, m_2 \text{ are defined in the proof of this}$$

theorem.

Proof Let us first define a set $D = \{(x, y) : m_1 < x < M_1, m_2 < y < M_2\}$, where $m_1, m_2 > 0$ and $0 < M_1, M_2 < \infty$, obviously D is compact in $\mathbb{R}^2$ and using the transformation

$$x(t) = x^* e^{v_1(t)}, \qquad y = y^* e^{v_2(t)}.$$

Therefore, the system (5) becomes

$$
\begin{cases}
\dfrac{dv_1}{dt} = \dfrac{(1 + ky)x^*(e^{v_1(t)} - 1)}{(1 + ky)(1 + ky^*)} - \dfrac{kxy^*(e^{v_2(t)} - 1)}{(1 + ky)(1 + ky^*)} + \dfrac{m(a + x^{*2})x^* y^*(e^{v_2(t)} - 1)}{(a + x^2)(a + x^{*2})} \\[3mm]
\qquad + \dfrac{m(a + x^{*2})x^* y^*(e^{v_1(t)} - 1)}{(a + x^2)(a + x^{*2})} - r_1 x^*(e^{v_1(t)} - 1), \\[3mm]
\dfrac{dv_2}{dt} = \dfrac{am\beta x^*(e^{v_1(t-\tau)} - 1)(x(t - \tau) + x^*)}{(a + x^2(t - \tau))(a + x^{*2})}.
\end{cases}
\tag{26}
$$

The above transformation changes the interior equilibrium points E^* to $(0, 0)$ in $v_1 - v_2$ plane. Let $V_1 = |v_1(t)|$ then computing the upper Dini derivative of $V_1(t)$ along the system (5), we obtain that,

$$
\begin{aligned}
D^+ V_1(t) &\leq \frac{(1 + kM_2)x^*|(e^{v_1(t)} - 1)|}{(1 + km_2)(1 + ky^*)} - \frac{km_1 y^*|(e^{v_2(t)} - 1)|}{(1 + kM_2)(1 + ky^*)} \\
&\quad + \frac{m(a + x^{*2})x^* y^*|(e^{v_2(t)} - 1)|}{(a + m_1^2)(a + x^{*2})} \\
&\quad + \frac{m(a + x^{*2})x^* y^*|(e^{v_1(t)} - 1)|}{(a + m_1^2)(a + x^{*2})} - r_1 x^*|(e^{v_1(t)} - 1)| \\
&\leq - \left[r_1 x^* - \frac{m(a + x^{*2})x^* y^*}{(a + m_1^2)(a + x^{*2})} - \frac{(1 + kM_2)x^*}{(1 + km_2)(1 + ky^*)} \right] |(e^{v_1(t)} - 1)| \\
&\quad - \left[\frac{km_1 y^*}{(1 + kM_2)(1 + ky^*)} - \frac{m(a + x^{*2})x^* y^*}{(a + m_1^2)(a + x^{*2})} \right] |(e^{v_2(t)} - 1)|.
\end{aligned}
$$

Now, we consider the functional as

$$V_{22}(t) = V_2(t) + \frac{2M_1^2 \beta m}{a} \int_{t-\tau}^{t} \int_{x}^{t} \left[\left(\frac{1}{(a + x^{*2})(a + M_1)} \right) x^* |e^{v_1(s-\tau)} - 1| \right] ds dx.$$

Therefore,

$$D^+ V_{22}(t) = D^+ V_2(t) + \frac{2\tau M_1^2 \beta m}{a} \left[\left(\frac{1}{(a+x^{*2})(a+M_1)} \right) x^* \left| e^{v_1(t-\tau)} - 1 \right| \right]$$

$$- \frac{2 M_1^2 \beta m}{a} \int_{t-\tau}^{t} \left[\left(\frac{1}{(a+x^{*2})(a+M_1)} \right) x^* \left| e^{v_1(s-\tau)} - 1 \right| \right] ds$$

$$\leq D^+ V_2(t) + \frac{2\tau M_1^2 \beta m}{a} \left[\left(\frac{1}{(a+x^{*2})(a+M_1)} \right) x^* \left| e^{v_1(t-\tau)} - 1 \right| \right]$$

$$\leq \left(a^2 + \tau \right) \frac{2 M_1^2 \beta m}{a(a+x^{*2})} x^* \left| e^{v_1(t} - 1 \right|.$$

Now, construct a Lyapunov functional $V(t) = V_1(t) + V_{22}(t) > |v_1(t)| + |v_2(t)|$.

Now, we calculate the upper right-hand derivative of $V(t)$ along with the solutions of the system (5), we get

$$D^+ V(t) = D^+ V_1(t) + D^+ V_{22}(t)$$

$$\leq - \left[r_1 x^* - \frac{m(a+x^{*2})x^* y^*}{(a+m_1^2)(a+x^{*2})} - \frac{(1+kM_2)x^*}{(1+km_2)(1+ky^*)} \right.$$

$$\left. - \left(a^2 + \tau \right) \frac{2 M_1^2 \beta m}{a(a+x^{*2})} x^* \right] |(e^{v_1(t)} - 1)|$$

$$- \left[\frac{km_1 y^*}{(1+kM_2)(1+ky^*)} - \frac{m(a+x^{*2})x^* y^*}{(a+m_1^2)(a+x^{*2})} \right] |(e^{v_2(t)} - 1)|$$

$$\leq -p_1 x^* |(e^{v_1(t)} - 1)| - p_2 y^* |(e^{v_2(t)} - 1)|,$$

where, $p_1 = r_1 - \dfrac{m(a+x^{*2})y^*}{(a+m_1^2)(a+x^{*2})} - \dfrac{(1+kM_2)}{(1+km_2)(1+ky^*)} - \left(a^2 + \tau \right) \dfrac{2 M_1^2 \beta m}{a(a+x^{*2})}, p_2 = $

$\dfrac{km_1}{(1+kM_2)(1+ky^*)} - \dfrac{m(a+x^{*2})x^*}{(a+m_1^2)(a+x^{*2})}.$

Since the model system (5) is permanent, then, for all $t > T$, we have $x^* e^{v_1(t)} = x(t) \geq m_1$, $y^* e^{v_2(t)} = x(t) \geq m_2$.

Now, we applying the mean value theorem, we get

$$x^* |e^{v_1(t)}| = x^* e^{\theta_1} |v_1(t)| > m_1 |v_1(t)|,$$

$$y^* |e^{v_2(t)}| = y^* e^{\theta_2} |v_2(t)| > m_2 |v_2(t)|,$$

where, $x^* e^{\theta_1(t)}$ lies between x^* and $x(t)$; $y^* e^{\theta_2(t)}$ lies between y^* and $y(t)$. Therefore, $D^+ V(t) \leq p_1 m_1 |v_1(t)| - c_2 m_2 |v_2(t)| \leq -\rho(|v_1(t)| + |v_2(t|)$, where $\rho = \min\{p_1 m_1, p_2 m_2\}$. Therefore, the coexisting equilibrium point E^* of the delayed model (5) will be globally asymptotically stable if $\min\{p_1 m_1, p_2 m_2\} > 0$. $\qquad\square$

4.4 Direction and stability of Hopf-bifurcation

Now, in this section we discuss the direction and stability of the coexisting equilibrium point through Hopf-bifurcation. To verify the direction of Hopf-bifurcation and stability of equilibrium points we shall use the center manifold theorem and normal form (Hassard et al.

1981). In the previous section, we see that, when τ crosses the critical value τ^* then the system (5) has experience the Hopf-bifurcation.

Now, consider the transformation $X_1(t) = x(t) - x^*$, $X_2(t) = y(t) - y^*$ and $\tau = \tau^* + \mu$, $\mu \in \mathbb{R}$, therefore, $\mu = 0$ is a Hopf-bifurcation value of the transferred model. Using the above transformation the system (5) transformed into

$$\dot{X}(t) = L_\mu(X_t) + g(\mu, X_t), \tag{27}$$

where $X(t) = (X_1(t), X_2(t))^T \in \mathbb{R}^2$. For $\psi = (\psi_1, \psi_2)^T \in \mathbf{C}([-1, 0], \mathbb{R}_+^2)$; $L_\mu : \mathbf{C} \to \mathbb{R}$ and $g : \mathbb{R} \times \mathbf{C} \to \mathbb{R}$ are given by

$$L_\mu(\psi) = (\tau^* + \mu)A^{(0)}\begin{pmatrix}\psi_1(0)\\\psi_2(0)\end{pmatrix} + (\tau^* + \mu)A^{(1)}\begin{pmatrix}\psi_1(-1)\\\psi_2(-1)\end{pmatrix} \tag{28}$$

and $g(\mu, \psi) = (\tau^* + \mu)A^{(2)}$, where $A^{(0)} = \begin{pmatrix}b_1 & b_2\\0 & b_5\end{pmatrix}$, $A^{(1)} = \begin{pmatrix}0 & 0\\b_3 & b_4\end{pmatrix}$, $A^{(2)} = \begin{pmatrix}q_1\psi_1^2(0) + q_2\psi_1(0)\psi_2(0) + q_3\psi_2^2(0)\\q_4\psi_1^2(-1) + q_5\psi_1(-1)\psi_2(-1)\end{pmatrix}$,

$$q_1 = \frac{my^*a(a - 3x^{*2})}{(x^{*2} + a)^3};$$

$$q_2 = -\frac{rk(ky^* + 1)}{(ky^* + 1)^3} - \frac{2amx^*}{(x^{*2} + a)^2};$$

$$q_3 = \frac{rk^2x^*}{(ky^* + 1)^3};$$

$$q_4 = \frac{\beta amy^*(a - 3x^{*2})}{(x^{*2} + a)^3};$$

$$q_5 = \frac{2\beta mx^*a}{(x^{*2} + a)^2}.$$

After that the Riesz representation theorem, there exist two dimensional matrix $\eta(\phi, \mu)$ are function of bounded variation such that

$$L_\mu\psi = \int_{-1}^{0} d\eta(\phi, \mu)\psi(\phi), \ for \ \psi \in \mathbf{C}, \tag{29}$$

where $\phi \in [-1, 0]$. Now, we choose $\eta(\phi, \mu) = (\tau^* + \mu)A^{(0)}\delta(\phi) - (\tau^* + \mu)A^{(1)}\delta(\phi + 1)$, where δ is the Dirac delta function and it is defined as

$$\delta(\phi) = \begin{cases}1, & \phi = 0,\\0, & \phi \neq 0.\end{cases}$$

For $\psi \in \mathbf{C}^1([-1, 0], \mathbb{R}_+^2)$, define

$$H(\mu)\psi = \begin{cases}\dfrac{d\psi(\phi)}{d\phi} & \phi \in [-1, 0]\\\int_{-1}^{0} d\eta(\mu, p)\psi(p) & \phi = 0.\end{cases} \quad and \quad R(\mu)\psi = \begin{cases}0 & \phi \in [-1, 0]\\g(\mu, \psi) & \phi = 0.\end{cases}$$

Then the system (27) becomes

$$\dot{X}_t = H(\mu)X_t + R(\mu)X_t \tag{30}$$

where $X_t(\phi) = X_t(t + \phi)$ for $\phi \in [-1, 0]$. For $\nu \in \mathbf{C}^1([0, 1], (\mathbb{R}_+^2)^*)$, define

$$H^*\nu(p) = \begin{cases} -\dfrac{d\nu(p)}{dp}, & p \in (0, 1], \\ \int_{-1}^0 d\eta^T(t, 0)\nu(-t), & p = 0, \end{cases}$$

and the bilinear inner product is given below

$$\langle \nu(p), \psi(\phi) \rangle = \bar{\nu}(0)\psi(0) - \int_{-1}^0 \int_{\gamma=0}^\phi \bar{\nu}(\gamma - \phi)d\eta(\phi)\psi(\gamma)d\gamma, \tag{31}$$

where $\eta(\phi) = \eta(\phi, 0)$.

Now, when $\mu = 0$ i.e. $\tau = \tau^*$ then the system (27) experiences the Hopf-bifurcation about the interior equilibrium point E^*. After that we use the eq. (28), we can say the characteristic equation of the system (27) has a pair of imaginary roots $\pm i\omega_0\tau^*$.

Clearly $H(0)$ and H^* are adjoint operators. Here, $\pm i\omega_0\tau^*$ are the eigenvalues of $H(0)$, so $\pm i\omega_0\tau^*$ are eigenvalues of H^*. After that, we will find the eigenvectors of $H(0)$ and H^* for the eigenvalue $i\omega_0\tau^*$ and $-i\omega_0\tau^*$ respectively.

Now, we consider that $q(\phi) = (1, \alpha_1)^T e^{i\omega_0\tau^*\phi}$ and $q^*(p)$ be the eigenvectors of $H(0)$ and H^* corresponding to the eigenvalues of $i\omega_0\tau^*$ and $-i\omega_0\tau^*$ respectively. Therefore we have $H(0)q(\phi) = i\omega_0\tau^*q(\phi)$. After that we use the definition of $H(0)$ and eq. (29), we find that $\tau^* \begin{pmatrix} b_1 - i\omega_0 & b_2 \\ b_3 e^{-i\omega_0\tau^*} & b_4 e^{-i\omega_0\tau^*} + b_5 - i\omega_0 \end{pmatrix} q(0) = \begin{pmatrix} 0 \\ 0 \end{pmatrix}$.

Therefore we get $q(0) = (1, \alpha_1)^T$ and $q^*(p) = D(1, \alpha_1^*)^T e^{i\omega_0\tau^*p}$,

where $\alpha_1 = \dfrac{b_3 e^{-i\omega_0\tau^*}}{-b_4 e^{-i\omega_0\tau^*} - b_5 + i\omega_0}$ and $\alpha_1^* = -\dfrac{b_2}{b_4 e^{i\omega_0\tau^*} + b_5 + i\omega_0}$. Now we choose the value of D such that $\langle q^*(p), q(\phi) \rangle = 1$ and $\langle q^*(p), \bar{q}(\phi) \rangle = 0$ as $D = \dfrac{1}{1 + \bar{\alpha}_1\alpha_1^* + (b_3 + b_4\bar{\alpha}_1)\alpha_1^*\tau^*e^{i\omega_0\tau^*}}$.

After that we will defined the center manifold C_0 at $\mu = 0$. Now we use the same way which is introduce by Hassard to compute the coordinates of the manifold.

Let us first assume that X_t be the solution of the eq. (30) when $\mu = 0$.

Define

$$Z(t) = \langle q^*, x_t \rangle, \quad W(t, \phi) = X_t(\phi) - 2Re\{Z(t)q(\phi)\}. \tag{32}$$

On the center manifold C_0, we have

$$W(t, \phi) = W(Z(t), \bar{Z}(t), \phi) = W_{20}(\phi)\frac{Z^2}{2} + W_{11}(\phi)Z\bar{Z} + W_{02}(\phi)\frac{\bar{Z}^2}{2}$$
$$+ W_{30}(\phi)\frac{Z^3}{6} + ...,$$

where Z and $\bar{Z}$ are the local coordinates along q^* and $\bar{q}^*$ of the center manifold C_0 respectively. Also W is real when X_t is real. Now $\mu = 0$, then the solution $X_t \in C_0$ of the eq. (30) is

$$\dot{Z}(t) = i\omega_0\tau^*Z + \langle \bar{q}^*(\phi), F(0, W(Z, \bar{Z}, \phi) + 2Re\{Zq(\phi)\}) \rangle$$
$$= i\omega_0\tau^*Z + \bar{q}^*(0)F(0, W(Z, \bar{Z}, 0) + 2Re\{Zq(0)\}) = i\omega_0\tau^*Z + \bar{q}^*(0)F_0(Z, \bar{Z}),$$

so this equation can be written as in the form $\dot{Z} = i\omega_0\tau^* + l(Z, \bar{Z})$ with

$$l(Z, \bar{Z}) = \bar{q}^*(0)F_0(Z, \dot{Z}) = l_{20}\frac{Z^2}{2} + l_{11}Z\bar{Z} + l_{02}\frac{\bar{Z}^2}{2} + l_{21}\frac{Z^2\dot{Z}}{2} + ..., \tag{33}$$

Then from the eq. (32) we have

$$X_t(\phi) = (X_{1t}(\phi), X_{2t}(\phi)) = W\left(Z(t), \bar{Z}(t), \phi\right) + 2Re\{Z(t)q(\phi)\}) \tag{34}$$

$$= W_{20}(\phi)\frac{Z^2}{2} + W_{11}(\phi)Z\bar{Z} + W_{02}(\phi)\frac{\bar{Z}^2}{2} + (1, \alpha_1)^T e^{i\omega_0\tau^*\phi}Z$$

$$+ (1, \bar{\alpha}_1)^T e^{-i\omega_0\tau^*\phi}\bar{Z} + O(|(Z, \bar{Z})|^3).$$

$$X_{1t}(0) = Z + \bar{Z} + W_{20}^1(0)\frac{Z^2}{2} + W_{11}^1(0)Z\bar{Z} + W_{02}^1(0)\frac{\bar{Z}^2}{2} + O(|(Z, \bar{Z})|^3)$$

$$X_{1t}(-1) = e^{-i\omega_0\tau^*}Z + e^{-i\omega_0\tau^*}\bar{Z} + W_{20}^1(-1)\frac{Z^2}{2} + W_{11}^1(-1)Z\bar{Z}$$

$$+ W_{02}^1(-1)\frac{\bar{Z}^2}{2} + O(|(Z, \bar{Z})|^3)$$

$$X_{2t}(0) = \alpha_1 Z + \bar{\alpha}_1\bar{Z} + W_{20}^2(0)\frac{Z^2}{2} + W_{11}^2(0)Z\bar{Z} + W_{02}^2(0)\frac{\bar{Z}^2}{2} + O(|(Z, \bar{Z})|^3)$$

$$X_{2t}(-1) = e^{-i\omega_0\tau^*}\alpha_1 Z + e^{-i\omega_0\tau^*}\bar{\alpha}_1\bar{Z} + W_{20}^2(-1)\frac{Z^2}{2} + W_{11}^2(-1)Z\bar{Z}$$

$$+ W_{02}^2(-1)\frac{\bar{Z}^2}{2} + O(|(Z, \bar{Z})|^3). \tag{35}$$

Then from the eq. (33) we can find

$$l(Z, \bar{Z}) = \bar{q}^*(0)F_0(Z, \bar{Z})$$

$$= \bar{D}(1, \bar{\alpha}_1^*)\tau^* \begin{pmatrix} q_1 X_{1t}^2(0) + q_2 X_{1t}(0)X_{2t}(0) + q_3 X_{2t}^2(0) \\ q_4 X_{1t}^2(-1) + q_5 X_{1t}(-1)X_{2t}(-1) \end{pmatrix}$$

$$= \bar{D}\tau^* q_1\{Z + \bar{Z} + W_{20}^1(0)\frac{Z^2}{2} + W_{11}^1(0)Z\bar{Z} + W_{02}^1(0)\frac{\bar{Z}^2}{2} + O(|(Z, \bar{Z})|^3)\}^2$$

$$+ \bar{D}\tau^* q_2\{Z + \bar{Z} + W_{20}^1(0)\frac{Z^2}{2} + W_{11}^1(0)Z\bar{Z} + W_{02}^1(0)\frac{\bar{Z}^2}{2} + O(|(Z, \bar{Z})|^3)\}$$

$$\times \{\alpha_1 Z + \bar{\alpha}_1\bar{Z} + W_{20}^2(0)\frac{Z^2}{2} + W_{11}^2(0)Z\bar{Z} + W_{02}^2(0)\frac{\bar{Z}^2}{2} + O(|(Z, \bar{Z})|^3)\}$$

$$+ \bar{D}\tau^* q_3\{\alpha_1 Z + \bar{\alpha}_1\bar{Z} + W_{20}^2(0)\frac{Z^2}{2} + W_{11}^2(0)Z\bar{Z} + W_{02}^2(0)\frac{\bar{Z}^2}{2} + O(|(Z, \bar{Z})|^3)\}^2$$

$$+ \bar{D}\tau^* \alpha_1^* q_4\{e^{-i\omega_0\tau^*}Z + e^{-i\omega_0\tau^*}\bar{Z} + W_{20}^1(-1)\frac{Z^2}{2}$$

$$+ W_{11}^1(-1)Z\bar{Z} + W_{02}^1(-1)\frac{\bar{Z}^2}{2} + O(|(Z, \bar{Z})|^3)\}^2$$

$$+ \bar{D}\tau^* \alpha_1^* q_5\{e^{-i\omega_0\tau^*}Z + e^{-i\omega_0\tau^*}\bar{Z} + W_{20}^1(-1)\frac{Z^2}{2}$$

$$+ W_{11}^1(-1)Z\bar{Z} + W_{02}^1(-1)\frac{\bar{Z}^2}{2} + O(|(Z, \bar{Z})|^3)\}$$

$$\times \{e^{-i\omega_0\tau^*}\alpha_1 Z + e^{-i\omega_0\tau^*}\bar{\alpha}_1\bar{Z} + W_{20}^2(-1)\frac{Z^2}{2}$$

$$+ W_{11}^2(-1)Z\bar{Z} + W_{02}^2(-1)\frac{\bar{Z}^2}{2} + O(|(Z, \bar{Z})|^3)\}$$

Now, we comparing this above equation with the coefficient of (33) we get

$$l_{20} = 2\bar{D}\tau^*[q_1 + q_2\alpha_1 + q_3\alpha_1 + q_4\alpha_1^* e^{-2i\omega_0\tau^*} + q_5\alpha_1\alpha_1^* e^{-2i\omega_0\tau^*}]$$

$$l_{11} = \bar{D}\tau^*[2q_1 + q_2\Re(\alpha_1) + 2q_3\alpha_1\bar{\alpha}_1 + 2\alpha_1^* e^{-2i\omega_0\tau^*} + q_5\alpha_1^* e^{-2i\omega_0\tau^*}\Re(\alpha_1)]$$

$$l_{02} = 2\bar{D}\tau^*[q_1 + q_2\bar{\alpha}_1 + q_3\bar{\alpha}_1 + q_4\alpha_1^* e^{-2i\omega_0\tau^*} + q_5\bar{\alpha}_1\alpha_1^* e^{-2i\omega_0\tau^*}]$$

$$l_{21} = \bar{D}\tau^*[2q_1\left(W_{20}^1(0) + 2W_{11}^1(0)\right) + q_2\left(2W_{11}^2(0) + W_{20}^2(0) + \bar{\alpha}_1 W_{20}^1(0) + 2\alpha_1 W_{11}^1\right)$$
$$+ 2q_3\left(W_{20}^2(0) + 2W_{11}^2(0)\right) + 2q_4\alpha_1^* e^{-i\omega\tau^*}\left(W_{20}^1(-1) + 2W_{11}^1(-1)\right)$$
$$+ q_5\alpha_1^* e^{-i\omega_0\tau^*}\left(2W_{11}^2(-1) + W_{20}^2(-1) + \bar{\alpha}_1 W_{20}^1(-1) + \alpha_1 W_{11}^1(-1)\right)]$$

Now, we find the values of $W_{20}(\omega)$ and $W_{11}(\omega)$. It is follows form the eqs. (30) and (32) that

$$\dot{W} = \dot{X}_t - \dot{Z}q - \dot{\bar{Z}}\bar{q} = \begin{cases} HW - 2Re\{\bar{q}^*(0)F_0q(\phi)\}, & \phi \in [-1, 0), \\ HW - 2Re\{\bar{q}^*(0)F_0q(\phi)\} + F_0, & \phi = 0 \end{cases} \tag{36}$$

$$= HW + N(Z, \bar{Z}, \phi), \tag{37}$$

where

$$N(Z, \bar{Z}, \phi) = N_{20}(\phi)\frac{Z^2}{2} + N_{11}(\phi)Z\bar{Z} + N_{02}(\phi)\frac{\bar{Z}^2}{2} + ... \tag{38}$$

After that we expand this above series and comparing the coefficients, we can get

$$(H - i2\omega_0\tau^*)W_{20}(\phi) = -N_{20}(\phi), \quad HW_{11}(\phi) = -N_{11}(\phi) \tag{39}$$

Now, from eq. (36) we see that for $\phi \in [-1, 0)$,

$$N(Z, \bar{Z}, \phi) = -\bar{q}^*(0)F_0q(\phi) - q^*\bar{F}_0\bar{q}(\phi) = -lq(\phi) - \bar{l}\bar{q}(\phi). \tag{40}$$

After that, if we compare the above coefficient with (38), we get

$$N_{20}(\phi) = -l_{20}q(\phi) - \bar{l}_{02}\bar{q}(\phi) \tag{41}$$

and

$$N_{11}(\phi) = -l_{11}q(\phi) - \bar{l}_{11}\bar{q}(\phi). \tag{42}$$

Now from (39) and (41), we have

$$\dot{W}_{20}(\phi) = i2\omega_0\tau^* W_{20}(\phi) + l_{20}q(\phi) + \bar{l}_{02}\bar{q}(\phi).$$

Since $q(\phi) = (1, \alpha_1)^T e^{i\omega_0\tau^*\phi}$, therefore we have

$$W_{20}(\phi) = \frac{il_{20}}{\omega_0\tau^*}q(0)e^{i\omega_0\tau^*\phi} + \frac{i\bar{l}_{20}}{3\omega_0\tau^*}\bar{q}(0)e^{-i\omega_0\tau^*\phi} + E_1 e^{i2\omega_0\tau^*\phi}, \tag{43}$$

where $E_1 = (E_1^{(1)}, E_1^{(2)}) \in \mathbb{R}^2$ be the constant vector.

Again from eqs. (39) and (42) give the following relation

$$W_{11}(\phi) = -\frac{il_{11}}{\omega_0\tau^*}q(0)e^{i\omega_0\tau^*\phi} + \frac{i\bar{l}_{11}}{\omega_0\tau^*}\bar{q}(0)e^{-i\omega_0\tau^*\phi} + E_2, \tag{44}$$

where E_2 is a constant vector. Now, we shall find the actual value for E_1 and E_2 in (43) and (44), respectively. Using the definition of H and eq. (39), we get

$$\int_{-1}^{0} d\eta(\phi)W_{20}(\phi) = i2\omega_0\tau^* W_{20}(0) - N_{20}(0) \tag{45}$$

and

$$\int_{-1}^{0} d\eta(\phi) W_{11}(\phi) = -N_{11}(0) \tag{46}$$

where $\eta(\phi) = \eta(0, \phi)$. From (39), we have

$$N_{20}(0) = -l_{02}q(0) - \bar{l}_{02}\bar{q}(0) + 2\tau^* \begin{pmatrix} q_1 + q_2\alpha_1 + q_3 \\ q_4 e^{-i\omega_0\tau^*} + q_5\alpha_1 e^{-i\omega_0\tau^*} \end{pmatrix} \tag{47}$$

and

$$N_{11}(0) = -l_{11}q(0) - \bar{l}_{11}\bar{q}(0) + 2\tau^* \begin{pmatrix} q_2\Re\{\phi\} \\ q_5\Re\{\phi\}e^{i\omega_0\tau^*} \end{pmatrix}. \tag{48}$$

Again noting that

$$\left(i\omega_0\tau^* I - \int_{-1}^{0} e^{i\omega\tau^*\phi} d\eta(\phi) \right) q(0) = 0,$$

and

$$\left(-i\omega_0\tau^* I - \int_{-1}^{0} e^{-i\omega\tau^*\phi} d\eta(\phi) \right) \bar{q}(0) = 0.$$

After that we substitute (43) and (47) into (45), we get

$$\left(i2\omega_0\tau^* I - \int_{-1}^{0} e^{i2\omega\tau^*\phi} d\eta(\phi) \right) E_1 = 2\tau^* \begin{pmatrix} q_1 + q_2\alpha_1 + q_3 \\ q_4 e^{-i\omega_0\tau^*} + q_5\alpha_1 e^{-i\omega_0\tau^*} \end{pmatrix},$$

which that

$$\begin{pmatrix} -b_1 + 2i\omega_0 & -b_2 \\ -b_3 e^{-2i\omega_0\tau^*} & -b_5 - b_4 e^{-2i\omega_0\tau^*} + 2i\omega_0 \end{pmatrix} E_1 = 2 \begin{pmatrix} q_1 + q_2\alpha_1 + q_3 \\ q_4 e^{-i\omega_0\tau^*} + q_5\alpha_1 e^{-i\omega_0\tau^*} \end{pmatrix} \tag{49}$$

which is implies that

$$E_1^{(1)} = \frac{|\Gamma_{11}|}{|\Gamma_1|}, \qquad E_1^{(2)} = \frac{|\Gamma_{12}|}{|\Gamma_1|}, \tag{50}$$

where

$$\Gamma_{11} = 2 \begin{pmatrix} q_1 + q_2\alpha_1 + q_3 & -b_2 \\ q_4 e^{-i\omega_0\tau^*} + q_5\alpha_1 e^{-i\omega_0\tau^*} & -b_5 - b_4 e^{-2i\omega_0\tau^*} + 2i\omega_0 \end{pmatrix},$$

$$\Gamma_{12} = 2 \begin{pmatrix} -b_1 + 2i\omega_0 & q_1 + q_2\alpha_1 + q_3 \\ -b_3 e^{-2i\omega_0\tau^*} & q_4 e^{-i\omega_0\tau^*} + q_5\alpha_1 e^{-i\omega_0\tau^*} \end{pmatrix},$$

$$\Gamma_1 = \begin{pmatrix} -b_1 + 2i\omega_0 & -b_2 \\ -b_3 e^{-2i\omega_0\tau^*} & -b_5 - b_4 e^{-2i\omega_0\tau^*} + 2i\omega_0 \end{pmatrix}.$$

Again from (44) , (48) and (46), we get

$$\left(\int_{-1}^{0} d\eta(\phi) \right) E_2 = 2\tau^* \begin{pmatrix} q_2\Re\{\phi\} \\ q_5\Re\{\phi\}e^{i\omega_0\tau^*} \end{pmatrix},$$

implies that

$$\begin{pmatrix} b_1 & b_2 \\ b_3 & b_5 + b_4 \end{pmatrix} E_2 = -2 \begin{pmatrix} q_2\Re\{\phi\} \\ q_5\Re\{\phi\}e^{i\omega_0\tau^*} \end{pmatrix},$$

and hence,

$$E_2^{(1)} = \frac{|\Gamma_{21}|}{|\Gamma_2|}, \qquad E_2^{(2)} = \frac{|\Gamma_{22}|}{|\Gamma_2|}, \qquad (51)$$

where

$$\Gamma_{21} = 2\begin{pmatrix} -q_2\Re\{\phi\} & b_2 \\ -q_5\Re\{\phi\}e^{i\omega_0\tau^*} & b_4+b_5 \end{pmatrix}, \Gamma_{22} = 2\begin{pmatrix} b_1 & -q_2\Re\{\phi\} \\ b_3 & -q_5\Re\{\phi\}e^{i\omega_0\tau^*} \end{pmatrix}, \Gamma_2 = \begin{pmatrix} b_1 & b_2 \\ b_3 & b_5+b_4 \end{pmatrix}.$$

We can then determine the values of $W_{20}(0)$ and $W_{11}(0)$ based on (44) and (45), respectively. Therefore, the delay and other biological parameters can be used to determine each value of l_{ij}. Lastly, we can compute the coefficients as follows:

$$C_1(0) = \frac{i}{2\omega_0\tau^*}\left(l_{20}l_{11} - 2|l_{11}|^2 - \frac{1}{3}|l_{02}|^2 + \frac{1}{2}l_{21}\right),$$

$$\mu_2 = -\frac{Re\{C_1(0)\}}{Re\{\lambda^{'}(\tau^*)\}}, \qquad \beta_2 = 2Re\{C_1(0)\}, \qquad (52)$$

$$T_2 = -\frac{Im\{C_1(0)\} + \mu_2 Im\{\lambda^{'}(\tau^*)\}}{\omega_0\tau^*}. \qquad (53)$$

The direction of the Hopf bifurcation is depends on the sign of μ_2, if $\mu_2 > 0(< 0)$ then the Hopf bifurcation is supercritical (subcritical); the stability of the bifurcating periodic solution is depends on the sign of β_2, if $\beta_2 < 0(> 0)$ then the bifurcated periodic solutions are stable (unstable); the period of the bifurcating periodic solution is depends on the sign of T_2, if $T_2 > 0(< 0)$ then the period of the bifurcating periodic solution increases (decreases).

5 Numerical simulation

To demonstrate the validity of the theoretical findings derived in previous sections using numerical simulations, we choose empirical values of parameters for the system (4) as shown in Table 1. A range of parameter values are found in published articles as follows: $r \in [0.48, 1.1]$ (Majumdar et al. 2022; Mondal et al. 2022); $k \in [0.4, 5]$ (Mondal et al. 2022; Majumdar et al. 2022); $r_0 \in [0.01, 0.5]$ (Wang et al. 2016; Das and Samanta 2021); $r_1 \in [0.06, 0.28]$ (Mondal et al. 2022; Majumdar et al. 2022) 5;$m \in [0.9, 4.5]$ (Mondal et al. 2022, a); $a \in [0.4, 2]$ (Majumdar et al. 2021; Jiang et al. 2018); $d \in [0.01, 0.06]$ (Mondal et al. 2022, a); $\beta \in [0.38, 0.9]$ (Mondal et al. 2022a; Majumdar et al. 2022); $q \in [0.2, 1]$ (Majumdar et al. 2022; Dubey et al. 2018); $E \in [0.2, 0.76]$ (Majumdar et al. 2022; Chakraborty et al. 2012). Based on the listed range, we present the values of system parameters in Table 1. We shall investigate different types of bifurcations (transcritical, Hopf bifurcation) and local, global stability of system solutions about various equilibrium points. For the considered set of parametric values in Table 1, we observed that the system has three different types of equilibrium points (trivial, axial and interior) through various parametric conditions (see Fig. 1). In this article, our analysis is performed in two different parts : (a) analysis for $\tau = 0$, i.e., for non-delayed system, (b) analysis for different values of τ, i.e., analysis for delayed system. In biological point of view, fear effect parameter (k) and harvesting effort parameter (E) are most important parameters of the proposed model system (4). In theoretical sections, we observed that intrinsic growth rate of prey (r) plays significant role to change the dynamics of system about corresponding equilibrium points. At first we shall discuss all numerical

Table 1 The description and emfarcil values of system variables and parameters with their dimensions

Symbol	Biological meaning	Numerical value	Dimension
r	Prey intrinsic growth rate	0.8	$time^{-1}$
k	Level of fear effect	1	$biomass^{-1}$
r_0	Normal death rate of prey population	0.01	$time^{-1}$
r_1	Coefficient of intra-specific interference of prey	0.1	$time^{-1}$
d	Death rate of predator	0.05	$biomass^{-1}time^{-1}$
a	Environmental protection coffecient to the prey	1.2	$biomass^{-\frac{1}{2}}time^{-1}$
β	Conversion rate of prey into predator	0.5	$biomass^{-\frac{1}{2}}time^{-1}$
m	Predation rate of prey by predator	1.2	$time^{-1}$
E	Harvesting effort	0.2	$time^{-1}$
q	The catchability coefficient	0.8	$time^{-1}$
τ	Time delay	1	$time$

simulation for the non-delayed system i.e., for $\tau = 0$ and later for delayed system i.e., for $\tau > 0$.

(a) **Numerical analysis for non-delayed system** ($\tau = 0$) :

In this discussion, we see how the dynamics of system (4) change for varying biologically important parameters r and E separately. In Fig. 1, we have observed that growth rate prey (r) has an important role in the existence of various types of equilibrium points for different parametric restrictions of r. In Fig. 2, we have presented the one parameter bifurcation diagram with respect to r which is showing the stability-instability of different equilibrium points of the system (4) and other parameters of the system are fixed as in Table 1. It is clear from the Fig. 2 that in the range $0 \leq r \leq 0.01$ only trivial equilibrium point E_0 exists which is stable (the corresponding phase portrait and time series evolution of species are given by Fig. 3a-b). For $0.01 \leq r \leq 0.09038$, along with the trial equilibria an axial equilibrium point exists and the trivial equilibrium point exchanges its stability through transcritical bifurcation with the axial equilibria (see the Fig. 3 (c), (d) for the corresponding phase diagram and time series evolution). It is also observed that if we increase the value of r more from the value 0.09038, axial equilibrium point exchanges its stability through creation interior equilibrium point. Thus the system again experiences transcritical bifurcation at axial equilibrium point for the threshold value of $r = r_{[TC]} = 0.09038$ with respect to the parameter r (see Fig. 2). Thus, when the system goes through critical value $r = r_{[TC]} = 0.09038$, with trivial and axial equilibrium points an interior equilibrium point arises and the interior equilibrium point is stable spiral in nature. The corresponding phase diagram and time series evolution of the system for $r > r_{[TC]}$ are given by Fig. 3(e), (f).

Biologically, the growth rate of prey r is a significant parameter of the model system (4). We noticed that when prey growth rate is very low, any of the species do not exist, i.e., the system goes to extinction. But, if we increase the parameter prey growth rate r more, only prey species can survive and because of very low prey density, predator goes to extinction for not availability of food. For more higher value of prey growth rate both the species can survive with positive population density.

In the model system (4) another significant parameter is harvesting effort of predator. It has an important role on stability of feasible equilibrium points of the model system (4).
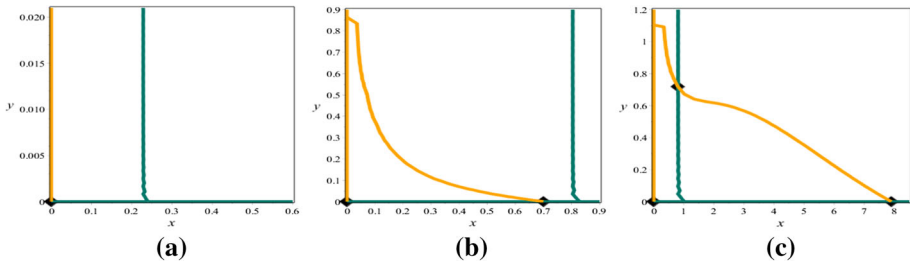
Fig. 1 The prey and predator nullclines for different parametric values of the prey intrinsic growth rate r like as: **a** existence of only trivial equilibrium point for the value of $r = 0.01$, **b** existence of trivial and axial equilibrium points for the value of $r = 0.08$ and **c** existence of trivial, axial and interior equilibrium points for the value of $r = 0.8$
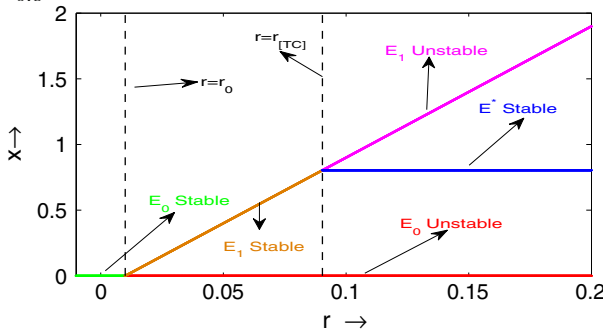

Fig. 2 This figure represent one dimensional bifurcation diagram with respect to prey intrinsic growth rate (r). The transcritical bifurcation occur at E_0 for threshold value $r = r_0 = 0.01$ and at E_1 for threshold value $r = r_{[TC]} = 0.09038$ where other values of parameters are taken from the Table 1. Also, in this figure green, grey, red, magenta and blue lines represent stable node, stable node, saddle point, unstable spiral and stable spiral of corresponding equilibrium points respectively.
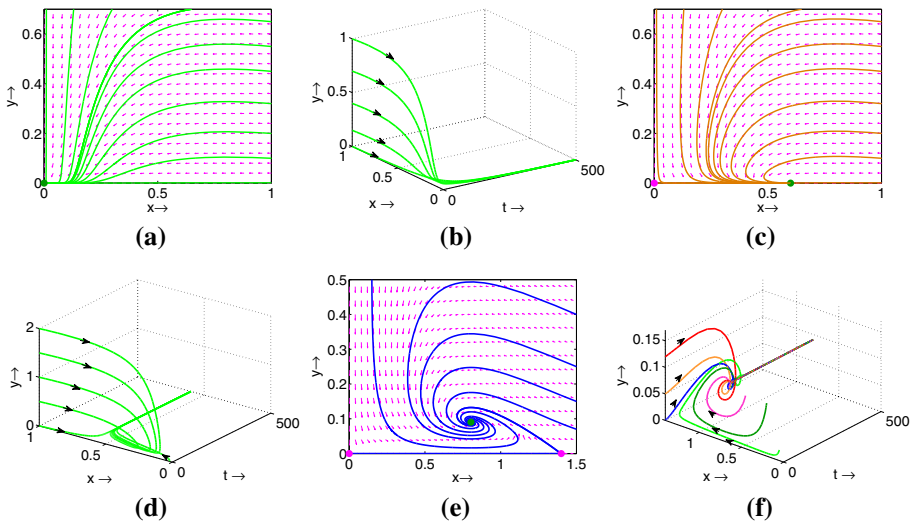
Fig. 3 These figures represent phase diagram with changing various values of prey intrinsic growth rate(r) and corresponding time series evolution of species for the model system (4) like as: **a, b** for the value of $r = 0.005$; **c), d** for the value of $r = 0.07$; **e, f** for the value of $r = 0.15$ when other values of parameters are choosen from the Table 1
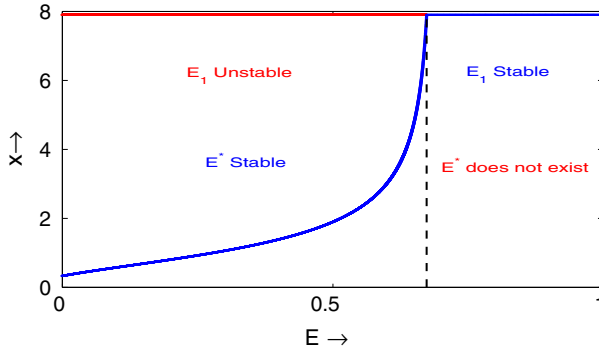
Fig. 4 This figure represent one dimensional bifurcation diagram with respect to the harvesting effort (E). The transcritical bifurcation occurs at E_1 for the threshold value $E = 0.67335$ while other values of the parameters are choosen from the Table 1. Also, blue and red lines corresponds to stable and unstable equilibrium points of the system. There are only two equilibrium points plotted here (E_1 and E^*), not plotted E_0, which is always present
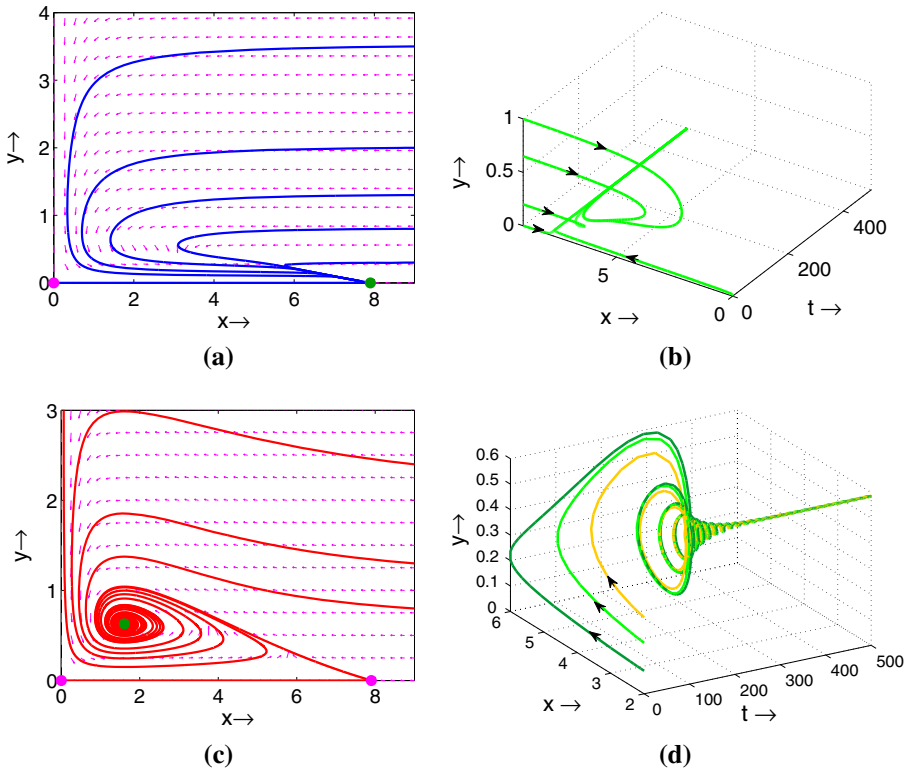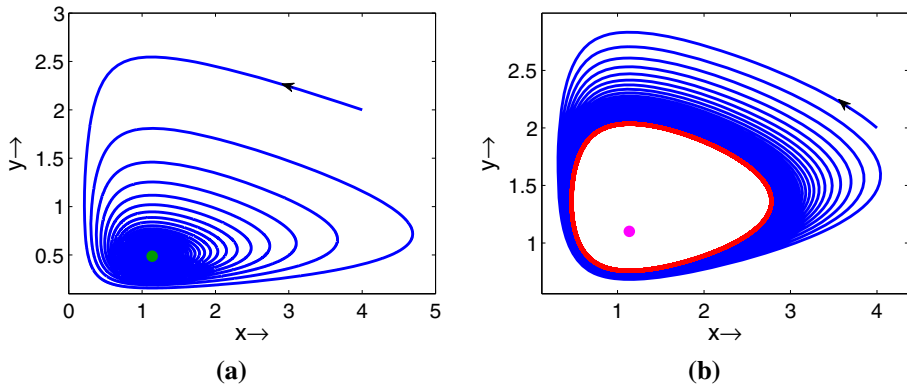

Fig. 5 These figures represent phase diagram with changing various values of harvesting effort parameter (E) and corresponding time series evolution of species for the model system (4) like as: **a, b** for the value of $E = 0.7$; **c, d** for the value of $E = 0.45$ when other values of parameters are choosen from the Table 1

Fig. 6 Phase diagram for two different values of the intrinsic growth rate parameter r of the model system (4) such as: **a** $r = 0.3$ for stable interior equilibrium point, **b** $r = 0.9$ for unstable interior equilibrium point with considering $r_1 = 0.01$, $m = 0.81$ and other parameters are same as in Table 1

It is clear from Fig. 4 that for $E > 0.67335$ the axial equilibrium point is stable and for $E < 0.67335$ the axial equilibria exchange its stability through the creation of an interior equilibrium point i.e., a transcritical bifurcation occurs when the parameter E passes through threshold value of $E = E^{[TC]} = 0.67335$ (other parameters are fixed in Table 1). Therefore, for $E < 0.67335$, trivial (which is always exist), axial and interior equilibrium exist. The stability nature of trivial equilibria is saddle, axial equilibria is saddle and interior equilibrium point is stable focus. Phase diagram and corresponding time series evolution are given by Fig. 5 (a), (b). Again, for $E > 0.67335$ the system has two equilibrium points (trivial, axial) and here the trivial equilibria is saddle and axial equilibria is stable node. This nature of the system is depicted by phase diagram and corresponding time series evolution Fig. 5 (c), (d).

From a biological point of view this behaviour is very meaningful because when harvesting effort is low, predator and prey density remains at a certain level to co-exist both species. But for higher harvesting effort, predator population will go to extinction and only prey species can survive. Thus the businessman has to be conscious on do not to cross the limit of harvesting for the survival of both species in the system.

Now, if we consider $r_1 = 0.01$, $m = 0.81$ and other parameters are taken from the Table 1, the system exhibits Hopf bifurcation at interior equilibrium point with respect to significant system parameters r, k and E. The parameter r experinces Hopf bifurcation when it passes through the threshold value $r = r^{[HB]} = 0.6010473853$. The stable and unstable phase diagram before and after the Hopf bifurcation are presented by Figs. 6(a) and 6(b), respectively.

The system (4) experiences Hopf bifurcation with respect to fear effect parameter k. The system undergoes Hopf bifurcation as it passes through critical value $k = k^{[HB]} = 1.729447669$ when values of system parameters are $r_1 = 0.01$, $m = 0.81$ and others are fixed in Table 1. The corresponding phase diagram before and after Hopf bifurcation are given by Fig. 7(a) for value of $k = 0.3$ and Fig. 7(b) for value of $k = 0.8$ respectively. Thus, the parameter k has high impact to change the system behaviour.

Again, the system experiences Hopf bifurcation two times with respect to the harvesting effort parameter E for threshold value $E = E^{[HB]} = 0.1982346549$ and $E = E^{[HB]} = 0.4399812534$. The system shows switching property by two times Hopf bifurcation with respect to the parameter E. Three different phase portraits for different values of E such as before the first Hopf bifurcation, between two Hopf bifurcations and after the second
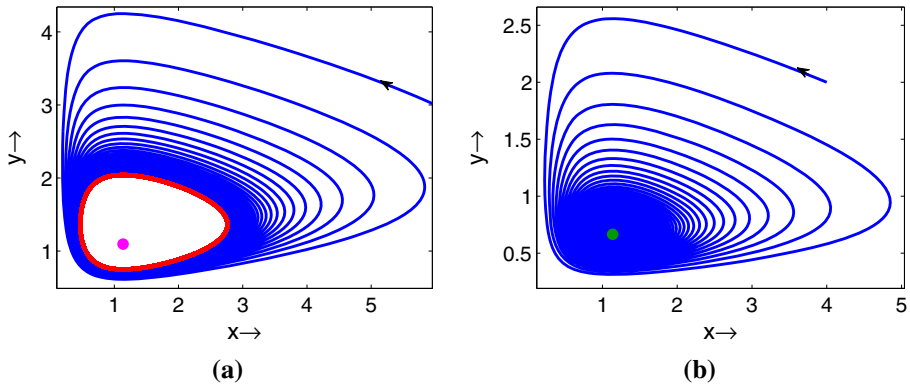
Fig. 7 Phase diagram for two different values of fear effect parameter k of the model system (4) such as: **a** $k = 0.8$ for unstable interior equilibrium point, **b** $k = 3$ for stable interior equilibrium point, considering $r_1 = 0.01$, $m = 0.81$ and other parameters are same as in Table 1
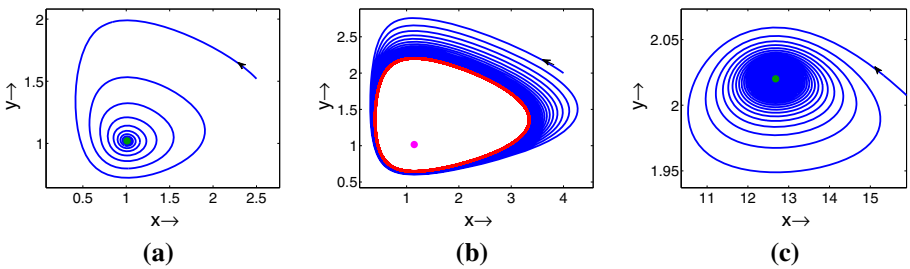

Fig. 8 Phase diagram for three different values of harvesting effort parameter E of the model system (4) such as: **a** $E = 0.17$ for stable interior equilibrium point, **b** $E = 0.202$ for unstable interior equilibrium point and **c** $E = 0.44$ for stable interior equilibrium point again, considering $r_1 = 0.01$, $m = 0.81$ and other parameters are same as in Table 1

Hopf bifurcation are given by Figs. 8 (a), 8 (b) and 8 (c). The biological significance of the parameter harvesting effort E is that the system shows switching behaviour with respect to the parameter E, which is most important in the biological aspect.

In Fig. 9 (a), (b) we have represented two dimensional projection of Hopf bifurcation curves in $E - r$ and $E - k$ parametric planes. In Fig. 9 (a), (b), green and orange coloured surfaces are showing stable and unstable regions for interior equilibrium point respectively. From Fig. 9 (a), we observed that for lower values of E, the interior equilibrium point is stable and from certain parametric values of E the interior equilibrium point is unstable. In this case, the impact of r is very low on stability of the interior equilibrium point of the system. Also for any value of r, the system enters into unstable region from the stable one when E crosses a certain critical value. Again, from Fig. 9 (b), we observed that impact of E and k both are high on stability of interior equilibrium point of the system. Here, for very higher values of k the system is stable when value of the E remains in a certain range. Thus, system parameters E and k both play important role on survive or destroy of species.

Now, we discuss the significance of system parameters on dynamics of population densities of the model system (4). In Fig. 10, we have presented the variation of population densities of both prey and predator species with respect to prey birth rate(r), conversion rate of prey into predator(β), and level of fear effect(k) respectively along with the change of the parameter
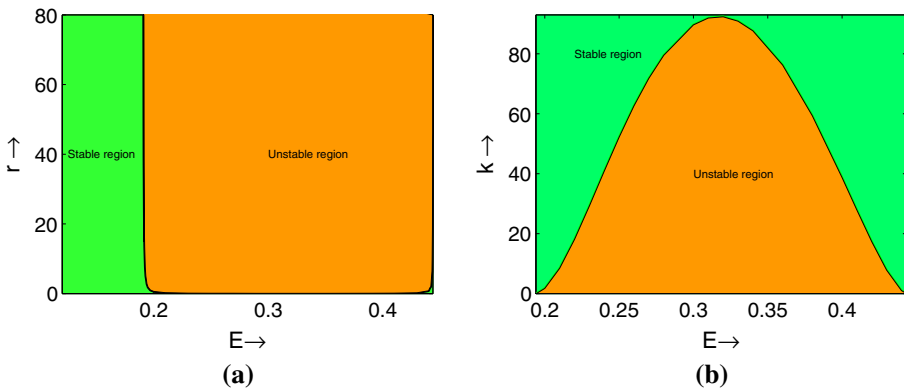
Fig. 9 These figures represent two dimensional projection of Hopf bifurcation curves for the system (4) in distinct parametric space, considering $r_1 = 0.01$, $m = 0.81$ and other parameters are taken from the Table 1

predator harvesting effort(E). With the increase of prey birth rate, prey density increases and consequently predator population density also increase. But the higher values of predator harvesting effort reduces the predator density in the system and increase the availability prey (see Fig. 10(a),(b)). If the system has a significantly good conversion rate of prey into predator, the predator density increase along with the decrease of prey density (see Fig. 10(c),(d)). We also observe that the level of fear effect decreases the amount of available prey in the environment and increase the predator density (see Fig. 10(e),(f)).

(b) **Numerical analysis for delayed system** ($\tau > 0$) :

In this section, fear effect of predator on prey (k) and time delay (τ) are very significant parameters. From ecological point of view, these two parameters are sensitive to change the dynamics of the system. Fixing other parameters as in Table 1, if we increase both values of k and τ the dynamics of the system change quickly. Here, we see that for lower values of delay parameter τ, the interior equilibria of system shows asymptotically stable behaviour. If we increase the value of τ more the interior equilibrium point becomes an unstable spiral and arise one periodic oscillation, then for further increasing τ, the oscillation becomes double-periodic and with the increase of the value τ many periodic oscillation or chaotic behaviour arise. In Fig. 11, green, orange, yellow and magenta coloured regions are denoted locally asymptotically stable region, solutions with one periodic oscillation, solutions with double-periodic oscillation and solutions with higher periodic or chaotic behaviour. Also, in this Fig. 11, the separatrix curve of blue and green lines depicts the Hopf bifurcation curve in the $k - \tau$ plane. Additionally, We also show one dimensional Hopf bifurcation curve of the system with respect to time delay parameter τ by the Fig. 12. Here, we see that the Hopf bifurcation occurs for threshold value of $\tau = 2.0325$. Moreover, in Fig. 13, we have presented a three dimensional Hopf bifurcation diagram with respect to the delay parameter τ. The blue and red-colored parts in this figure show the equilibrium point's stability and instability, and their intersection represents the Hopf bifurcation for this threshold value τ.

Now, in green region of Fig. 11, the interior equilibrium point is locally asymptotically stable and corresponding phase diagram and time series evolution are given by the Fig. 14 (a), (b). Then if we enter into orange region of Fig. 11, the nature of system solutions becomes one periodic oscillation which are depicted by Fig. 14 (c) ,(d). Next, in yellow region of Fig. 11, system solutions give double periodic oscillations and corresponding graphical representation are given by Fig. 14 (e), (f). Finally for very higher value of τ, i.e., in magenta
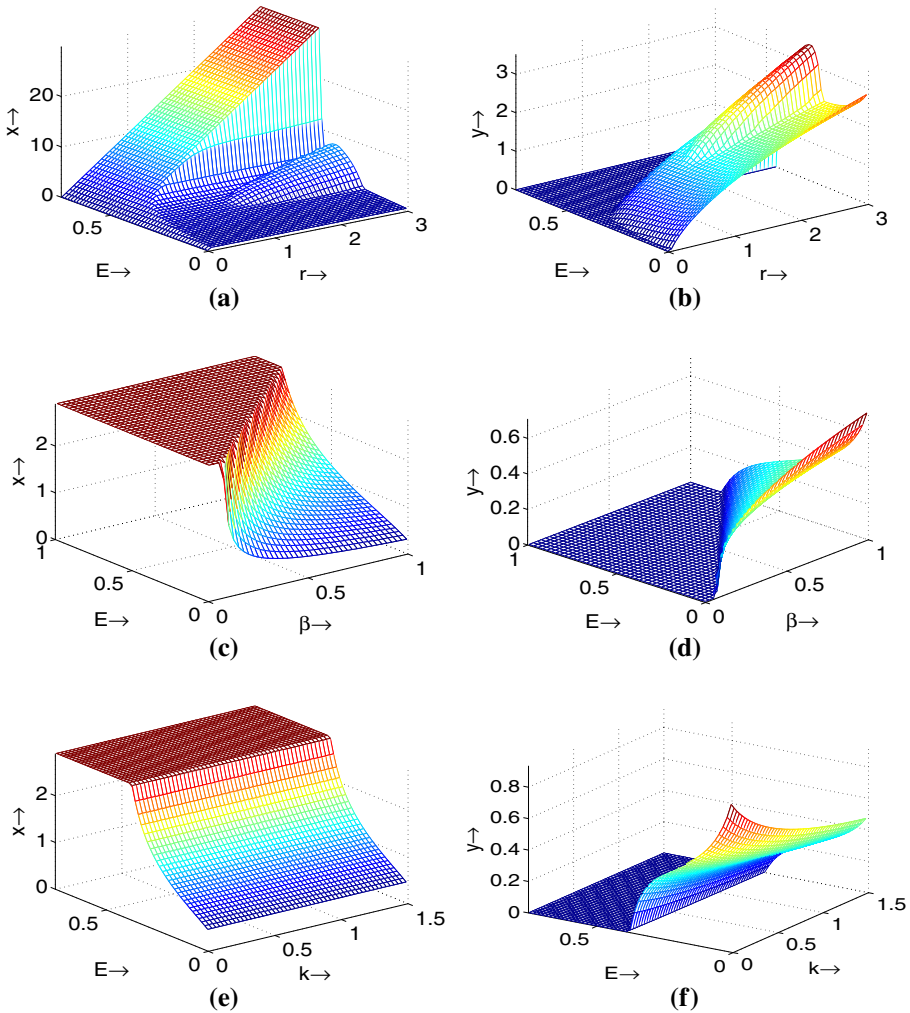
Fig. 10 Variations in population densities of prey(first column), and predator(second column) with respect to (**a**), (**b**) E and r; (**c**), (**d**) E and β and (**e**), (**f**) E and k when other values of parameters are chosen from the Table 1

coloured region of Fig. 11, solutions of the system give many periodic oscillation showing chaotic behaviour and the corresponding graphical representation are given by 14 (g), (h).

In Fig. 15, we have presented a three dimensional phase diagram by varying the delay parameter τ from 0 to 50. Blue, green, and red colors represent asymptotically stable spirals, limit cycles, and chaotic oscillations (or higher periodic oscillations). From this figure, it is clear that with increasing the value of τ, the system shows unstable behaviour with stable limit cycle, one periodic, two periodic, many periodic, or chaotic behavior from the stable of the equilibrium point.

Figure 16 depicts one dimensional bifurcation diagram of system (5) with respect to delay parameter τ (varying $\tau = 0$ to 50) when values of other parameters of the system are given in Table 1. The Fig. 16 describes one periodic, two periodic, many periodic and
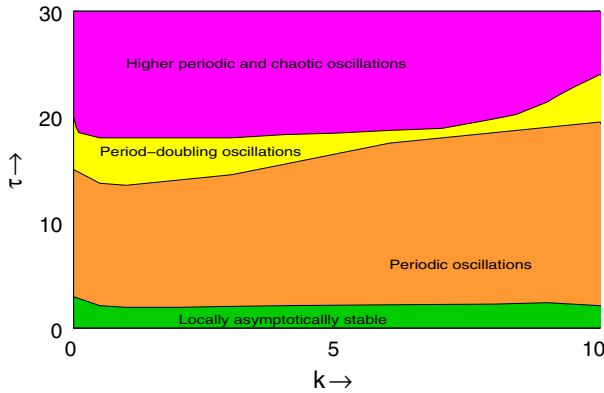
Fig. 11 Regions of stability or instability of the model system (5) in the $k - \tau$ parametric plane. Here green, orange, yellow and magenta regions indicate locally asymptotically stable region, solutions with one periodic oscillation, solutions with double-periodic oscillation and solutions with higher periodic or chaotic behaviour respectively
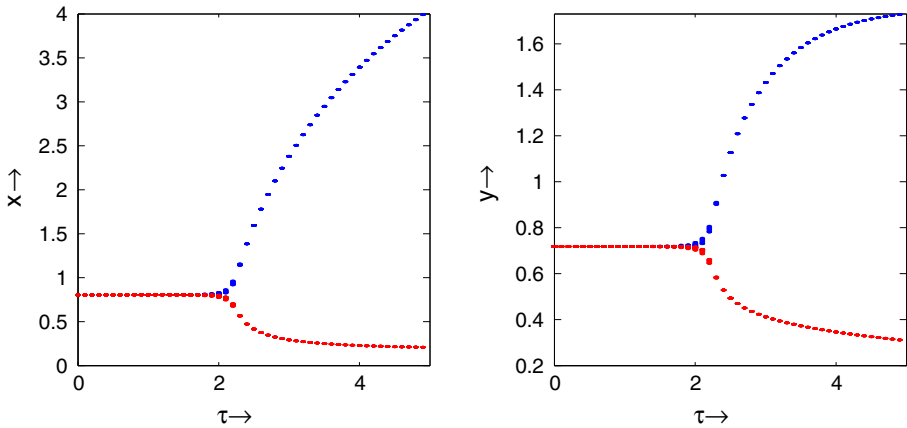

Fig. 12 Hopf bifurcation diagram with respect to time delay parameter τ of model system (5) when other parameters are fixed as given in Table 1

chaotic behaviour of solutions of the system. Here, the Hopf bifurcation or one periodic oscillation of solutions of the system occurs for the value of $\tau = \tau_0 = 2.0325$, two periodic oscillation of the solution occurs for $\tau = 13.324$ and many periodic solution or chaotic behaviour of the solution occurs for $\tau > 17.354$. Thus with the increase of parameter τ the dynamical behaviour of solutions of the system change through one period, two periods, many periods and finally chaotic and for the very lower value of τ the interior equilibria is locally asymptotically stable.

6 Conclusion and discussion

In this present article, we have proposed a two-dimensional prey-predator model where prey grows logistically and the birth rate of prey reduces due to the fear of the predator. It is assumed that predator consumes prey according to Holling type III functional response. Also,
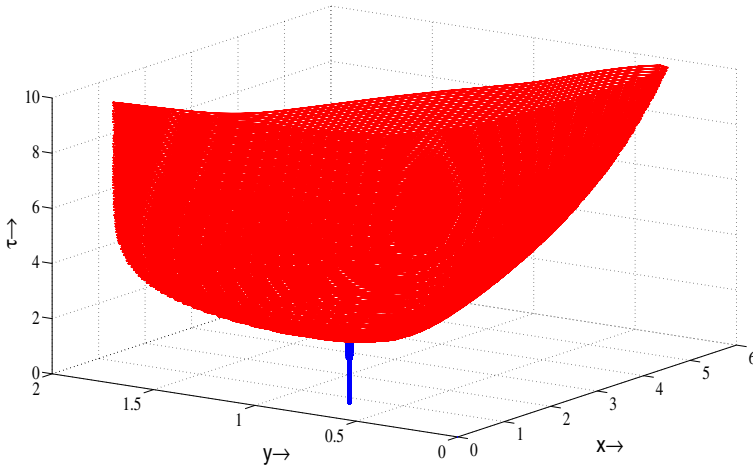
Fig. 13 This figure represents the three dimensional Hopf bifurcation diagram with respect to delay parameter τ when other value of parameters are taken from the Table 1. Here blue portion in the figure presents the interior equilibrium point is stable and in the red portion the interiornequilibrium point is unstable with stable limit cycle

predators are economically significant and harvested linearly. Further, we introduce gestation delay in the system to get much more realistic and richer dynamics. First, we study the model dynamics without introducing the delay parameter. The positivity and boundedness of system solutions have been established under certain parametric conditions. The system consists of three different types of equilibrium points, trivial, axial and coexistence equilibrium points. Local stability of all equilibrium points by using the eigenvalue analysis method has been discussed under different parametric conditions. The intrinsic growth rate of prey (r) plays an important role to change the dynamics of the system through transcritical bifurcation at both trivial and axial equilibrium points. Here, we observed that for the very lower, moderate and higher values of the intrinsic growth rate of prey both species go to extinction, predator goes to extinction and both species exist with positive density. Similarly, lower values of harvesting effort (E) both species exist with positive density and for higher values predator species goes to extinction. Again, we found that the system changes its stability through Hopf bifurcation with respect to the intrinsic growth rate of prey, fear effect parameter and harvesting effort. Additionally, the system shows switching property with changes of harvesting effort. We also observed that any nominal change in prey birth rate or conversion rate of prey into predator or level of fear effect along with the predator harvesting effort, the population density of both species change dramatically and the system may enter into the stable state from the unstable one and vise-versa.

In the delayed system we observed that the delay parameter (τ) has a high impact to change the system dynamics. For the delay parameter, the system changes its stability through Hopf bifurcation with arising a stable limit cycle. Also, we observed that the system arises one periodic, two periodic, higher periodic and chaotic oscillation with the increase of the value of delay parameter. Again, we found the effect of fear and delay in the $k - \tau$ plane. Here, the system shows stable, one periodic, two periodic, many periodic and chaotic for various values of fear and delay. In comparison of the non-delayed and delayed system, we observed that in the non-delayed system, the system arises only one periodic oscillation but for the delay, the system arises one periodic, two periodic, many periodic and chaotic oscillation.
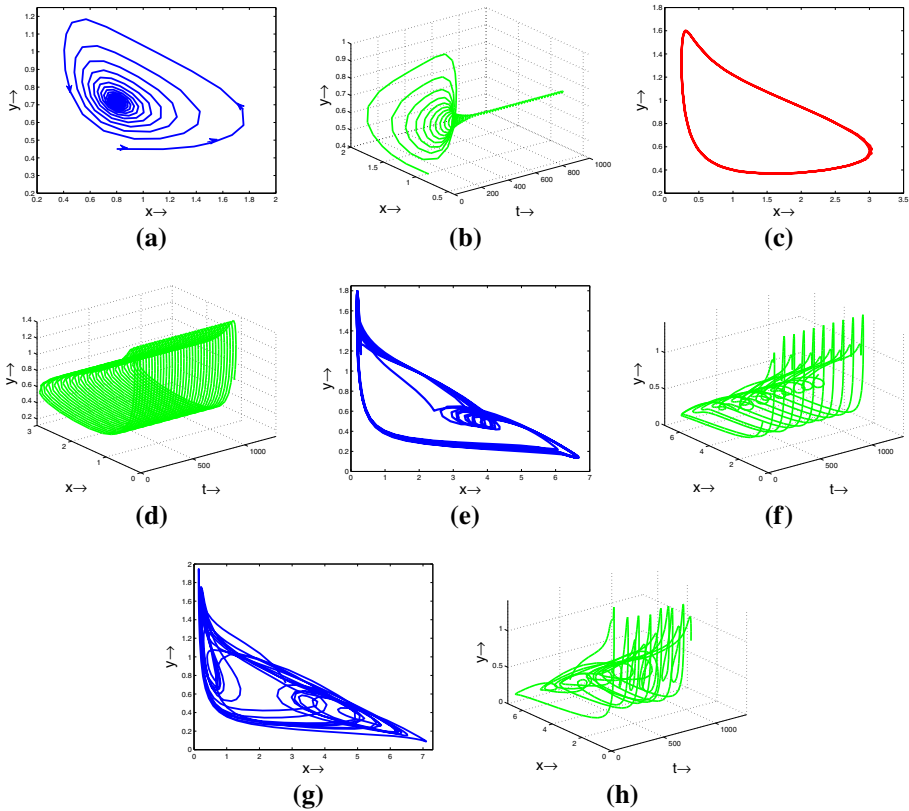
Fig. 14 These figures depict phase portrait diagram for separate values of parameter τ and corresponding time series evolution of species prey, predator for the model system (5) like as: **a**, **b** for the value of $\tau = 1.8$; **c**, **d** for the value of $\tau = 3.895$; **e**, **f** for the value of $\tau = 25$; **g**, **h** for the value of $\tau = 40$ when other values of parameters are chosen from the Table 1

Thus, the delay parameter has a high impact to change the stability dynamics of a system and hence bifurcation dynamics of the delayed model can be regulated by the significant delay parameter.

In Sk et al. (2022) authors showed that the fear of the middle predator creates stability while the fear of the top predator creates instability in a three-dimensional model. According to Xie and Zhang (2022), fear can stabilize the periodic system when considering the same functional response. By using numerical simulation in this paper, it has been shown that fear also stabilizes the system, but introducing gestation delay further makes it periodic with one or more periodicities. Finally, the model can be further extended by replacing the linear harvesting with the non-linear harvesting function, which will be more realistic and perspective of the biological diversity. This type of work is most commonly applicable to economically important species, such as marine sub ecosystems where harvesting provides financial support.
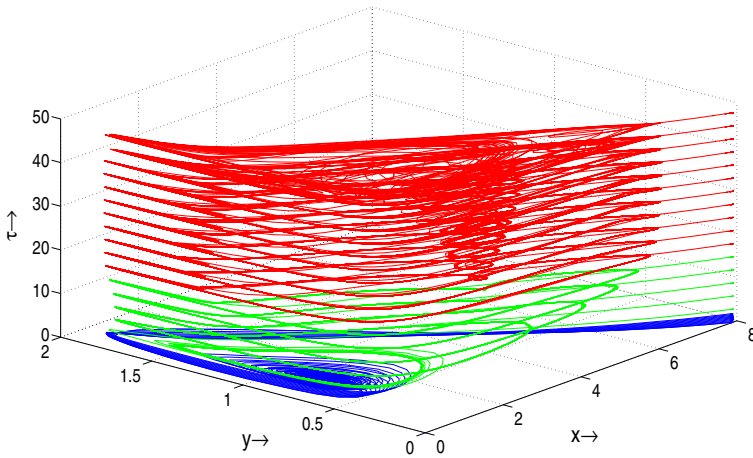
Fig. 15 This three dimensional figure represents the phase diagram of the model system (5) for variation of τ from 0 to 50 when other parameter values are same as Table 1. Here, the blue, green phase attractors describe that the interior equilibrium point is asymptotically stable spiral, stable limit cycle respectively and red attractors represent two periodic, four periodic and many periodic or chaotic osillation of the interior equilibrium point
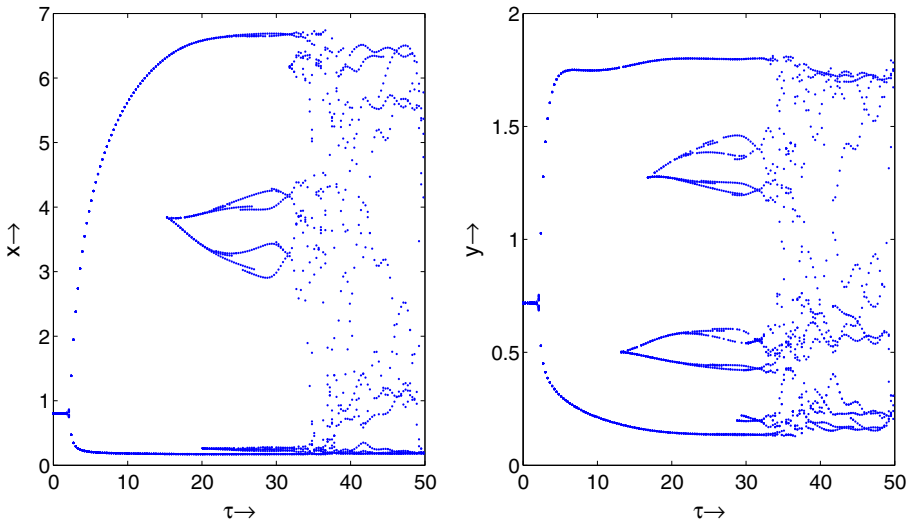

Fig. 16 Bifurcation diagram with respect to delay parameter τ for the model system (5) when values of other parameters are fixed in the Table 1. The first one is bifurcation diagram for prey and second one is bifurcation diagram for predator

Declarations

Data availability statements All data generated or analysed during this study are included in this article.

Conflict of interest Authors declare that he/she has no conflict of interest.

References

Allee WC (1931) Animal Aggregations: A Study in General Sociology. The University of Chicago Press, Chicago

Baek H (2010) A food chain system with Holling type IV functional response and impulsive perturbations. Comput Math Appl 60(5):1152–1163

Biswas S (2017) Optimal predator control policy and weak Allee effect in a delayed prey-predator system. Nonlinear Dyn 90:2929–2957

Chakraborty K, Jana S, Kar TK (2012) Global dynamics and bifurcation in a stage structured prey-predator fishery model with harvesting. Appl Math Comput 218(18):9271–9290

Collings JB (1997) The effects of the functinal response on the bifurcation behavior of a mite predator-prey interaction model. J Math Biol 036:149–168

Das A, Samanta GP (2021) Modelling the fear effect in a two-species predator-prey system under the influence of toxic substances. Rend Circ Mat Palermo 70(3):1501–1526

Das T, Mukherjee RN, Chaudhuri KS (2009) Bioeconomic harvesting of a prey-predator fishery. J Biol Dyn 3(5):447–462

Debnath S, Ghosh U, Sarkar S (2019) Global dynamics of a tritrophic food chain model subject to the Allee effects in the prey population with sexually reproductive generalized-type top predator. Comput Math Method 2(2):e1079

Debnath S, Majumdar P, Sarkar S, Ghosh U (2021) Chaotic Dynamics of a Tri-Topic Food Chain Model with Beddington-DeAngelis Functional Response in Presence of Fear Effect. Nonlinear Dyn. https://doi.org/10.1007/s11071-021-06896-0

Dubey B, Patra A, Upadhyay RK (2014) Dynamics of phytoplankton, zooplankton and fishery resource model. Appl Appl Math Int J (AAM) 9(1):14

Dubey B, Agarwal S, Kumar A (2018) Optimal harvesting policy of a prey-predator model with Crowley-Martin-type functional response and stage structure in the predator. Nonlinear Anal Model Cont 23(4):493–514

Ferdy JB, Austerlitz F, Moret J, Gouyon PH, Godelle B (1999) Pollinator-induced density dependence in deceptive species. Oikos 87:549–560

Freedman HI (1980) Deterministic Mathematical Models in Population Ecology. Marcel Dekker, New York

Ghosh U, Sarkar S, Mondal B (2021) Study of stability and bifurcation of three species food chain model with non-monotone functional response. Int J Appl Comput Math 7(63)

Gupta RP, Chandra P, Banerjee M (2015) Dynamical complexity of a prey-predator model with nonlinear predator harvesting. Discrete Contin Dyn Syst 20(2):423–443

Hassard BD, Hassard BD, Kazarinoff ND, Wan YH, Wan YW (1981) Theory and applications of Hopf bifurcation, CUP Archive, 41

Holling CS (1959) Some characteristics of simple types of predation and parasitism1. Canadian entomol 91(7):385–398

Holling CS (1965) The functional response of predators to prey density and its role in mimicry and population regulation. Mem Entomol Soc Can 45:5–60

Hu D, Cao H (2017) Stability and bifurcation analysis in a predator-prey system with Michaelis-Menten type predator harvesting. Nonlinear Anal Real World Appl 33:58–82

Jiang Z, Zhang W, Zhang J, Zhang T (2018) Dynamical analysis of a phytoplankton-zooplankton system with harvesting term and Holling III functional response. Int J Bifurc Chaos 28(13):1850162

Kempf A, Floeter J, Temming A (2008) Predator-prey overlap induced Holling type III functional response in the North Sea fish assemblage. Mar Ecol Prog Ser 367:295–308

Kuang Y (1993) Delay differential equations: with applications in population dynam- ics, 191. Academic Press

Kundu KUSUMIKA, Pal S, Samanta SUDIP, Sen A, Pal N (2018) Impact of fear effect in a discrete-time predator-prey system. Bull Calcutta Math Soc 110:245–264

Leeuwen EV, Jansen VAA, Bright PW (2007) How population dynamics shape the functional response in a one predator-two-prey system. Ecology 88(6):1571–1581

Lenzini P, Rebaza J (2015) Non-constant predator harvesting on a ratio dependent predator-prey model. Appl Math Sci 4:791–803

Lin CM, Ho CP (2006) Local and global stability for a predator-prey model of modified Leslie-Gower and Holling-type II time delay. Tunghai Sci 8:33–61

Lotka AJ (1925) Elements of physical biology. Baltimore, NY, Williams and Wilkins

Ma Z, Wang S (2018) A delay-induced predator-prey model with Holling type functional response and habitat complexity. Nonlinear Dyn 93(3):1519–1544

Majumdar P, Debnath S, Sarkar S, Ghosh U (2021) The complex dynamical behavior of a Prey-Predator model with holling Type-III functional response and non-Linear predator harvesting. Int J Model Simul. https://doi.org/10.1080/02286203.2021.1882148

Majumdar P, Debnath S, Mondal B, Sarkar S, Ghosh U (2022) Complex dynamics of a prey-predator interaction model with Holling type-II functional response incorporating the effect of fear on prey and non-linear predator harvesting. Rend Circ Mat Palermo 2:1–32

Majumdar P, Bhattacharya S, Sarkar S, Ghosh U (2022) On optimal harvesting policy for two economically beneficial species mysida and herring: a clue for conservation biologist through mathematical model. Int J Model Simul 1-23

Malthus TR (1872) An Essay on the Principle of Population

May RM (2001) Stability and Complexity in Model Ecosystems. Princeton University Press, New Jercy

Mondal B, Ghosh U, Rahman MS, Saha P, Sarkar S (2022) Studies of different types of bifurcations analyses of an imprecise two species food chain model with fear effect and non-linear harvesting. Math Comput Simul 192:111–135

Mondal B, Sarkar S, Ghosh U (2022) Complex dynamics of a generalist predator-prey model with hunting cooperation in predator. Eur Phys J Plus 137:43

Mondal B, Roy S, Ghosh U, Tiwari PK (2022) A systematic study of autonomous and nonautonomous predator-prey models for the combined effects of fear, refuge, cooperation and harvesting. Eur Phys J Plus 137(6):724

Morozov AY (2010) Emergence of Holling type III zooplankton functional response: bringing together field evidence and mathematical modelling. J Theo Biol 265(1):45–54

Murdoch WW (1977) Stabilizing effects of spatial heterogeneity in predator-prey systems. Theo Popul Biol 11(2):252–273

Murray JD (2002) Mathematical Biology I: An Introduction. Springer, Berlin

Onana M, Mewoli B, Tewa JJ (2020) Hopf bifurcation analysis in a delayed Leslie-Gower predator-prey model incorporating additional food for predators, refuge and threshold harvesting of preys. Nonlinear Dyn 100:3007–3028

Panday P, Pal N, Samanta S, Chattopadhyay J (2018) Stability and Bifurcation Analysis of a Three-Species Food Chain Model with Fear. Int J Bifurc Chaos 28:1850009

Panja P (2019) Prey-predator-scavenger model with Monod-Haldane type functional response. Rend Circ Mat Palermo 69(3):1205–1219

Peng G, Jiang Y, Li C (2009) Bifurcations of a Holling-type II predator-prey system with constant rate harvesting. Int J Bifur Chaos 19(08):2499–2514

Sarkar K, Khajanchi S (2020) Impact of fear effect on the growth of prey in a predator-prey interaction model. Ecol Complex 42:100826

Sen M, Banerjee M, Morozov A (2014) Stage-structured ratio-dependent predator-prey models revisited: When should the maturation lag result in systems' destabilization. Ecol Complex 19:23–34

Sk N, Tiwari PK, Pal S (2022) A delay nonautonomous model for the impacts of fear and refuge in a three species food chain model with hunting cooperation. Math Comput Simul 192:136–166

Volterra V (1926) Variazioni e Fluttuazioni del Numero d Individui in Specie Animali Conviventi, C. Ferrari, 31-113

Wang X, Zanette L, Zou X (2016) Modelling the fear effect in predator-prey interactions. J Math Biol 73:1179–1204

Wang X, Zanette L, Zou X (2016) Modelling the fear effect in predator-prey interactions. J Math Biol 73(5):1179–1204

Wangersky PJ, Cunningham WJ (1957) Time lag in prey-predator population models. Ecology 38:136–139

Xiao D, Jennings L (2005) Bifurcations of a Ratio-Dependent Predator-Prey System with Constant Rate Harvesting. SIAM J Appl Math 65(3):737–753

Xie B, Zhang N (2022) Influence of fear effect on a Holling type III prey-predator system with the prey refuge. AIMS Math 7(2):1811–1830

Zanette LY, White AF, Allen MC, Clinchy M (2011) Perceived predation risk reduces the number of offspring songbirds produce per year. Science 334:1398–1401

Zhang X, Chen L, Neumann AU (2000) The stage-structured predator-prey model and optimal harvesting policy. Math Biosci 168(2):201–210

Zhanga H, Cai Y, Fu S, Wan W (2019) Impact of the fear effect in a prey-predator model incorporating a prey refuge. Appl Math Comput 356:328–337